12

SYSTEMS, SCIENCE AND SOFTWARE

SSS-R-77-3194

SIMULATION AND DECOMPOSITION OF MULTIPLE EXPLOSIONS

D. G. LAMBERT
T. C. BACHE
J. M. SAVINO

TOPICAL REPORT

SPONSORED BY
ADVANCED RESEARCH PROJECTS AGENCY
ARPA ORDER No. 2551

This research was supported by the Advanced Research Projects Agency of the Department of Defense and was monitored by AFTAC/VSC, Patrick Air Force Base, Flordia, 32925, under Contract No. F08606-76-C-0041.

JUNE 1977

P. O. BOX 1620, LA JOLLA, CALIFORNIA 92038, TELEPHONE (714) 453-0060

AFTAC Project Authorization No. VELA/T/7712/B/ETR

Program Code No. 6H189

Effective Date of Contract: October 1, 1976

Contract Expiration Date: September 30, 1977

Amount of Contract: $410,412

Contract No. F08606-76-C-0041

Principal Investigator and Phone No.
Dr. Thomas C. Bache, (714) 453-0060, Ext. 337

Project Scientist and Phone No.
Dr. Ralph W. Alewine, III, (202) 325-8484

UNCLASSIFIED

SECURITY CLASSIFICATION OF THIS PAGE (When Data Entered)

REPORT DOCUMENTATION PAGE

READ INSTRUCTIONS BEFORE COMPLETING FORM

1. REPORT NUMBER	2. GOVT ACCESSION NO.
3. RECIPIENT'S CATALOG NUMBER	
4. TITLE (and Subtitle)	5. TYPE OF REPORT & PERIOD COVERED
SIMULATION AND DECOMPOSITION OF MULTIPLE EXPLOSIONS,	Topical Report.
	6. PERFORMING ORG. REPORT NUMBER
	SSS-R-77-3194
7. AUTHOR(s)	8. CONTRACT OR GRANT NUMBER(s)
D. G. Lambert T. C. Bache J. M. Savino	F08606-76-C-0041
9. PERFORMING ORGANIZATION NAME AND ADDRESS	10. PROGRAM ELEMENT, PROJECT, TASK AREA & WORK UNIT NUMBERS
Systems, Science and Software P. O. Box 1620 La Jolla, California 92038	Program Code No. 6H189 ARPA Order No. 2551
11. CONTROLLING OFFICE NAME AND ADDRESS	12. REPORT DATE
VELA Seismological Center 312 Montgomery Street Alexandria, Virginia 22314	June 1977
	13. NUMBER OF PAGES 66
14. MONITORING AGENCY NAME & ADDRESS (if different from Controlling Office)	15. SECURITY CLASS. (of this report) Unclassified
	15a. DECLASSIFICATION DOWNGRADING SCHEDULE

16. DISTRIBUTION STATEMENT (of this Report)

Approved for Public Release, Distribution Unlimited.

17. DISTRIBUTION STATEMENT (of the abstract entered in Block 20, if different from Report)

18. SUPPLEMENTARY NOTES

19. KEY WORDS (Continue on reverse side if necessary and identify by block number)

Seismology	Explosion Array
Simulated Multiple Exlosions	MAST
Close-in Seismograms	COLBY
Narrow-Band Filtering	POOL

20. ABSTRACT (Continue on reverse side if necessary and identify by block number)

The purpose of the study is to develop procedures for using seismic measurements to verify the number and yields of individual explosions making up a multiple event. Multiple explosion seismograms are simulated by straightforward summations of single explosion records. Several types of multiple explosions are simulated. These include closely spaced equal yield explosions (no consideration given to propagation path effects

OVER

DD FORM 1 JAN 73 1473 EDITION OF 1 NOV 65 IS OBSOLETE

388 507

UNCLASSIFIED

SECURITY CLASSIFICATION OF THIS PAGE (When Data Entered)

20. ABSTRACT (continued)

between explosions and receiver) and relatively more widely spaced explosions (propagation path effects included) of varying yields. The data employed are principally close-in seismic recordings of the Nevada Test Site explosions obtained from Sandia Laboratories in Albuquerque, New Mexico. Decomposition of the simulated multiple explosion records is accomplished using a series of narrow-band filters with center frequencies ranging from 3 to 100 Hz. In general, our results show that the narrow-band filter technique is able to achieve accurate time separation and amplitude scaling. The limitation on the technique is essentially the requirement for the presence of sufficient signal energy at frequencies greater than about 3.5 times the inverse of the lag time between arriving signals.

ABSTRACT

The purpose of the study is to develop procedures for using seismic measurements to verify the number and yields of individual explosions making up a multiple event. Multiple explosion seismograms are simulated by straightforward summations of single explosion records. Several types of multiple explosions are simulated. These include closely spaced equal yield explosions (no consideration given to propagation path effects between explosions and receiver) and relatively more widely spaced explosions (propagation path effects included) of varying yields. The data employed are principally close-in seismic recordings of the Nevada Test Site explosions obtained from Sandia Laboratories in Albuquerque, New Mexico. Decomposition of the simulated multiple explosion records is accomplished using a series of narrow-band filters with center frequencies ranging from 3 to 100 Hz. In general, our results show that the narrow-band filter technique is able to achieve accurate time separation and amplitude scaling. The limitation on the technique is essentially the requirement for the presence of sufficient signal energy at frequencies greater than about 3.5 times the inverse of the lag time between arriving signals.

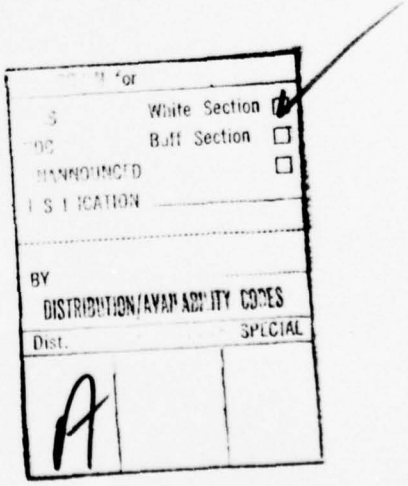

TABLE OF CONTENTS

TABLE OF CONTENTS (continued)

LIST OF ILLUSTRATIONS

LIST OF ILLUSTRATIONS (continued)

LIST OF TABLES

I. INTRODUCTION AND SUMMARY

This report is a continuation of earlier work concerning the separation and scaling of multiple explosions reported by Lambert, et al., [1976] and Savino, et al., [1976]. In this previous work close-in seismic records from MAST were used to simulate multiple explosions. Narrow-band filters were employed to separate and determine the relative sizes of the individual explosions making up the multiple explosion. These earlier results are reviewed in detail in this report.

The objective of the present study is to develop procedures for using seismic measurements to verify the number and yields of individual explosions making up a multiple event. We are also interested in how well our techniques are able to detect explosions detonated at the same time as the multiple event, but located outside the explosion array.

In this report we discuss three kinds of simulated multiple explosions. The first kind can be considered to be comprised of an array of three closely-spaced, equal-sized explosions observed along two close-in station arrays (Section III). For these composites we summed the individual station seismograms with themselves. Thus, we did not account for path differences between the individual explosions and the receiver. In Section VI we look at teleseismic recordings of multiple explosions of this kind. Application of the narrow-band filtering technique (frequency range from 3 to 100 Hz) to these simulations yielded the following significant results:

- Separation of the individual events was observed to begin at a characteristic frequency that is about 3.5 times the inverse of the explosion lag time. The explosion lag times ranged from 0.034 to 2.0 seconds in the several simulated events studied.

- Accurate separation and relative scaling of events is achieved as long as the signal-to-noise ratio is one or more at the aforementioned characteristic frequency. This requirement is most easily met at stations close to the event, since high frequency energy attenuates rapidly with distance. For single station teleseismic recordings the signal-to-noise ratio is such that separation of events with less than 2.0 second lags was not achieved.

The second kind of multiple event can be thought of as an array of four widely-spaced, equal-sized explosions observed at one close-in station. Such an event is simulated by summing seismograms from a linear array of stations that recorded one event. We think of the actual explosion epicenter as the recording station for our simulated event and the actual recording stations are then the epicenters of the events in our simulation. In this way the simulated event includes propagation path differences between the various sources and the receiver. Several such events were constructed and the application of the narrow-band filter technique (Section IV) gives the following results:

- The complexity of the later portion of the simulated event seismograms (i.e., slapdown times and later) increased as compared to those from the closely-spaced multiple event.

- Separation of events is achieved by analyzing the first portion of the composite signal. Accurate separation of events is obtained for those detected. Scaling of the detected events gives relative amplitudes varying by about a factor of two from the expected values. Occasionally, larger deviations occur and these are probably due to interference from other signal phases.

- There were two situations in which we were not able to detect an event; one in which the separation was only 0.05 seconds and one in which the main arrival occurred at the same time as the spall closure phase from an earlier event.

The third multiple event configuration is similar to that discussed above. However, we use recordings of several different events and thus introduce more complex propagation path effects as well as different explosion yields (Section V). This is the most complex class of simulated events we studied. The application of the narrow-band filtering technique produced results similar to those described above for the second configuration.

For the second two types of simulated events, the widely-spaced explosions, we are unable to realistically construct seismograms at more than one station. Thus, it is not possible to quantitatively evaluate the degree to which an array of stations will aid in the scaling problem. However, qualitatively, it seems clear that an array of stations should considerably improve the resolution of the technique. Tentatively identified events could be correlated from station to station and the signal-to-noise ratio may be improved upon processing data from an array. Even restricting attention to the single station data studied here, we are able to conclude that our narrow-band filter technique is able to identify and scale closely spaced arrivals from separate events. It should be emphasized that successful use of this technique requires the presence of sufficient signal energy at frequencies greater than 3.5 times the inverse of the separation time.

II. BASIC DATA

The data selected and used for simulating the various multiple explosion scenarios consist of close-in seismic measurements of the contained underground explosions MAST (June 19, 1975), COLBY (March 10, 1976) and POOL (March 17, 1976), all of which were detonated in the Pahute Mesa region at the Nevada Test Site (NTS). These data were obtained in digital format from Sandia Laboratories in Albuquerque, New Mexico and include accelerometer and velocity gauge seismograms recorded at horizontal ranges from approximately ground-zero to about 20 kilometers. The digital data were sampled at a rate of 500 points per second.

In the numerical simulations to be discussed, vertical component velocity data of the MAST, COLBY and POOL explosions are used. These records are shown in Appendix A. For simulating multiple explosions recorded at teleseismic distances we used the vertical component short-period seismogram from a single station (E) for MAST. In this particular case, the digital data were sampled at a rate of 20 points per second.

III. MULTIPLE EXPLOSION SIMULATION - CONSTRUCTION OF COMPOSITE SEISMOGRAMS FROM ONE GROUND MOTION RECORDING

This section of the report provides a summary of the important results gained from our previous work reported by Lambert, et al., [1976]. This simulation is the simplest and most easily understood of those we have done and is useful for describing the analytical methods used to decompose simulated multiple explosions time series. It is also useful for comparing to other, more complex, experiments.

3.1 STATION AND EVENT LOCATIONS

The explosion and recording configuration used for the first multiple event simulation are shown in Figure 1. This test consisted of a linear array of three equivalent yield explosions, equally spaced (355 m) and detonated simultaneously. The explosion spacing of 355 m was taken as representative of a row of cratering shots in the yield range near 150 kt.

For constructing seismograms, close-in velocity recordings of the MAST explosion were used. The simulated composite seismograms were constructed along the in-line and 45 degree profiles shown in Figure 1 by delaying and summing the actual MAST seismograms recorded at the (approximate) corresponding distances. The delays were based on the spacings between shots, the propagation velocity assumed and the azimuth to the recording station.

An example of a composite seismogram is given in Figure 2. This seismogram is for Station 3 along the in-line profile. On the left-hand side of Figure 2 we show the actual velocity record at Station 3 for MAST. The horizontal distance range is 0.912 km. The multiple explosion record is shown on the right-hand side of Figure 2. Comparing the original and

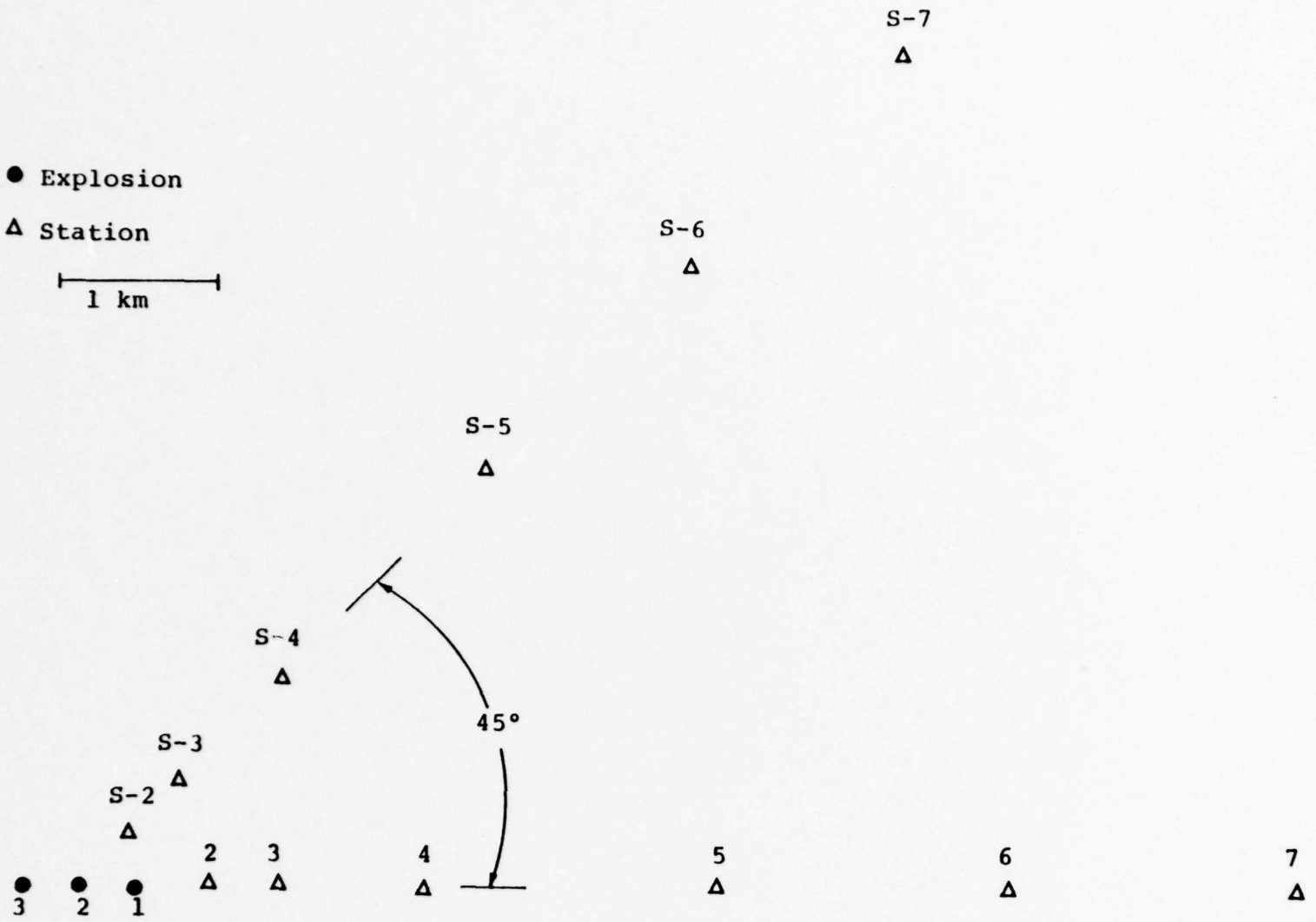

Figure 1. Simulated multiple explosion and station configuration.

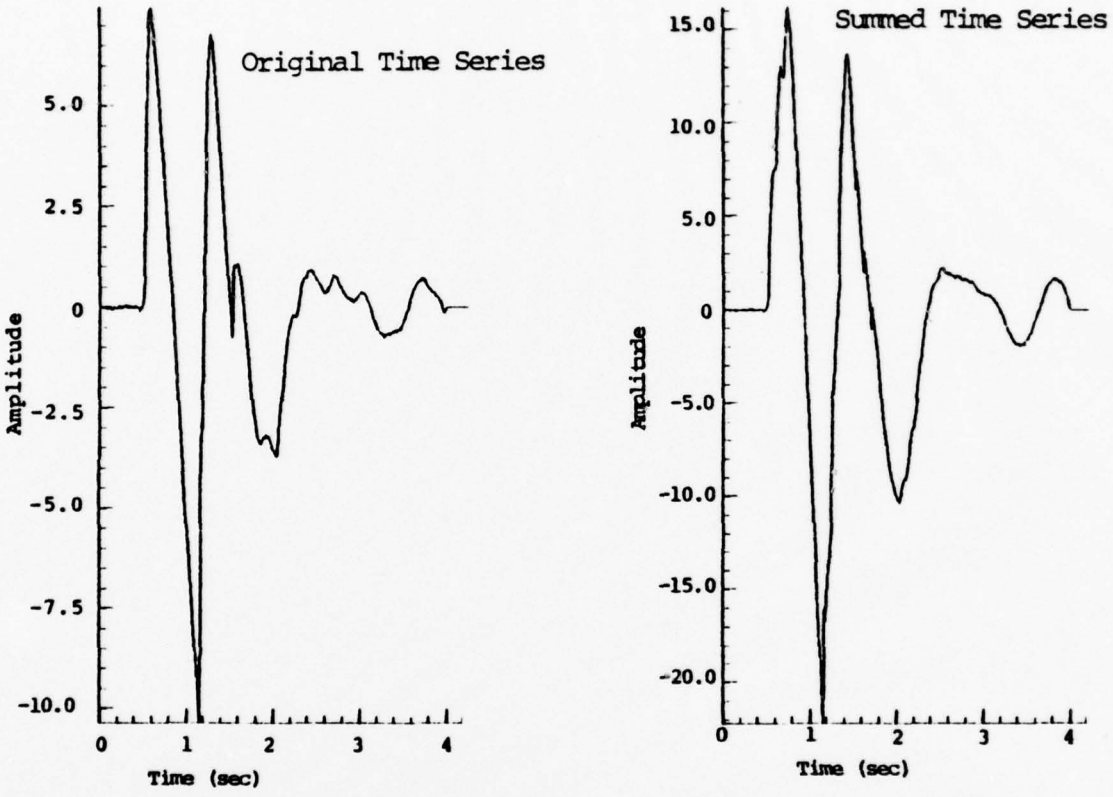

Figure 2. Original MAST signal recorded at Station 3 and composite signal corresponding to the same station along the profile in-line with the multiple shot array.

composite signals we see an expected increase in peak-to-peak signal amplitude and the superposition of the delayed signals from the three explosions. The latter effect is seen as only a subtle change in the shape of the waveform.

3.2 SIGNAL DECOMPOSITION FOR THE PROFILE OF STATIONS IN-LINE WITH THE EXPLOSION ARRAY

In Figure 2 we showed the original and composite seismogram for Station 3 located 0.912 km from MAST. The delay times are based on a 355 m spacing between the three shots and a velocity of 3.8 km/sec. Hence, delay times of 0.093 seconds are appropriate for all stations along the in-line profile.

A series of 16 narrow-band filters with center frequencies (f_c) ranging from 20 to 100 Hz were applied to both the original and composite signal shown in Figure 2. (For details of the MARS programs and description of the narrow-band filters used, see Appendix B). The time series output from these filters is shown in Figure 3. For the original MAST record at Station 3, three major bursts of high frequency energy occur for this band of frequencies (Figure 3a). The times are 0.55, 1.2 and 1.55 seconds. The time of first burst (0.55 sec) correlates with the first motion on the seismogram. The time of the second burst (0.12 sec) corresponds to the slap down phase. The third burst (1.55 sec) is more difficult to identify but seems to be a clear indication of a discrete arrival. Regardless of the origin of these high frequency bursts of energy, the important fact remains that there is a high signal-to-noise ratio at these frequencies. The significance of this result is shown in Figure 3b when the same set of filters is applied to the composite (three explosions) record. Here the three major bursts of energy now show triple peaks where before there was only one. Separation begins at about 40 Hz and becomes increasingly clear at higher frequencies.

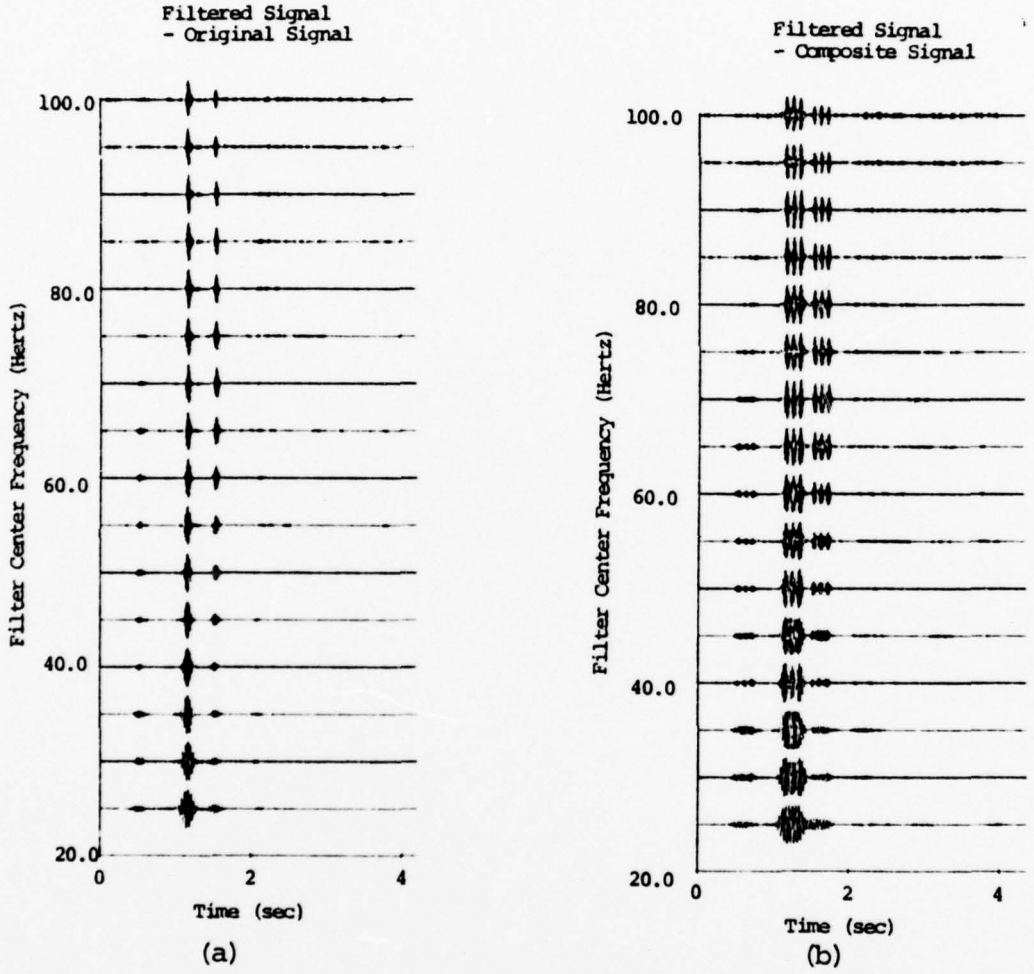

Figure 3. Narrow-band filtered signals (as functions of frequency and time) for the original (a) and composite (b) signals for Station 3 (Figure 2) along the profile in-line with the shot array.

Envelope functions were constructed for each of sixteen filter outputs using the Hilbert transform [Savino, et al., 1975]. The envelope functions are shown in Figure 4 for the original and composite signals. The important point to note (Figure 4b) is the clear separation of the three explosions making up the composite signal. The separation is even more dramatic in Figure 5b, where the sum of the envelopes at the different frequencies are plotted for the composite signal. A similar sum of the original signal is shown in Figure 5a for comparison.

The time separation of the three maximum power arrivals in Figure 5b corresponds closely to the time delays (0.093 seconds) for the three simulated explosions. Further, note that while the amplitude in the composite signal in Figure 2 is more than twice that of the original signal in Figure 2, each peak in the composite envelope sum is nearly equal in amplitude to the peak amplitude of the original unsummed signal (Figure 5).

Similar results are obtained for Stations 2 and 4 in this profile. Again, three major high frequency energy levels are observed. Separation of the three explosions becomes apparent at about 40 Hz and becomes more distinct with increasing frequency. The average time separation between the peaks is 0.093 seconds for both cases. The computed delay times for our decomposition correspond almost exactly to the actual delay times (Table 1).

For Stations 5, 6 and 7, high frequency noise dominates the records and the high frequency energy, if present, is too small to obtain any definitive results. Spectral analysis of the signal and a noise sample at Station 7 shows that the signal-to-noise ratio in the frequency range of 25 to 160 Hz is essentially one [Lambert, et al., 1976].

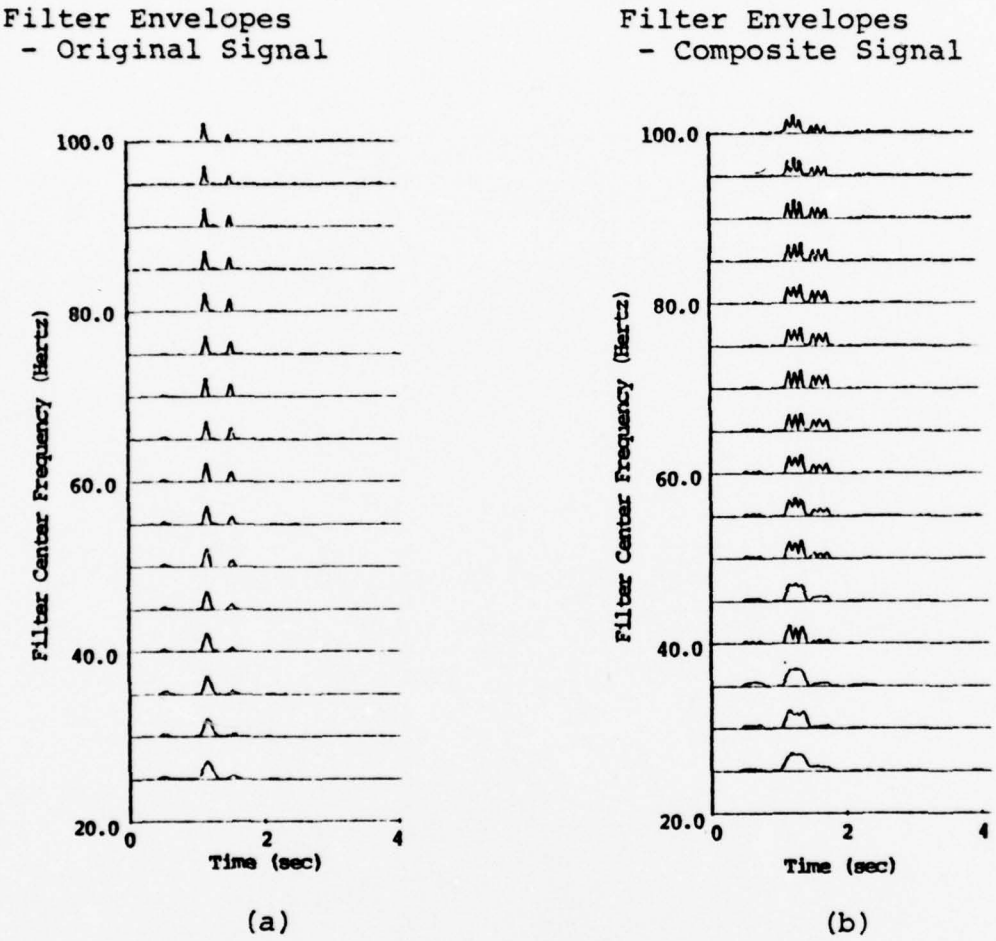

Figure 4. Envelope functions (as functions of frequency and time) for narrow-band filtered original (a) and composite (b) signals for Station 3 (Figure 1) along the profile in-line with the shot array.

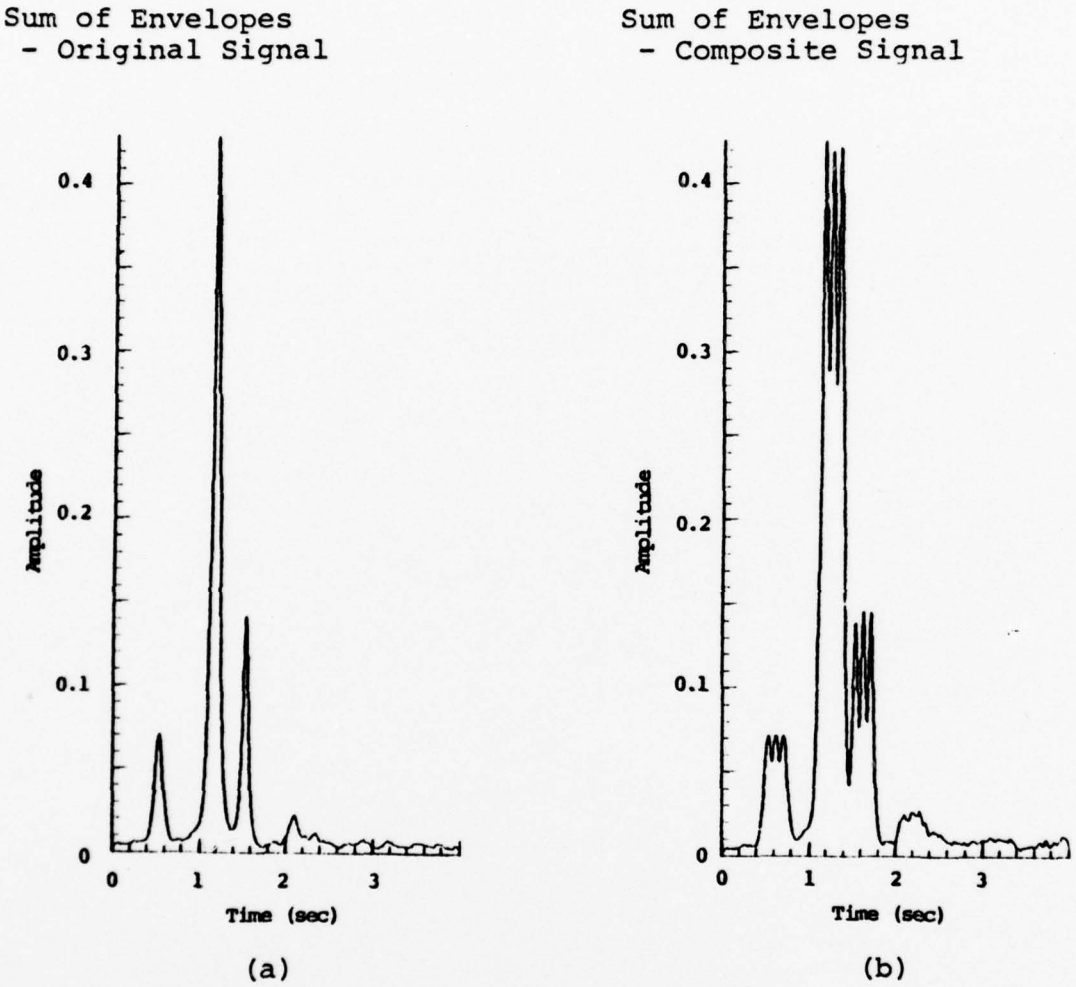

Figure 5. Sum of the envelopes shown in Figure 4 for the original (a) and composite (b) signals for Station 3 along the profile in-line with the shot array.

TABLE 1

ACTUAL DELAY TIMES VERSUS COMPUTED DELAY TIMES

Station \ Shot	Actual Delay Times For Stations In-Line With Shot Array (sec)		Computed Delay Times For Stations In-Line With Shot Array (sec)		Actual Delay Times For Stations Along 45° Profile Relative to Shot #2 (sec)		Computed Delay Times For Stations Along 45° Profile Relative to Shot #2 (sec)	
2	1-2 0.093	2-3 0.093	1-2 0.091	2-3 0.093	1-2 0.034	2-3 0.076	1-2 0.034	2-3 0.076
3	0.093	0.093	0.093	0.092	0.053	0.072	0.052	0.073
4	0.093	0.093	0.092	0.093	0.061	0.069	0.060	0.070
5	0.093	0.093	--	--	0.062	0.067	--	--
6	0.093	0.093	--	--	0.063	0.066	--	--
7	0.093	0.093	--	--	0.064	0.066	--	--

3.3 SIGNAL DECOMPOSITION FOR THE PROFILE 45° FROM THE EXPLOSION ARRAY

Composite or summed seismograms for the stations oriented at a 45° azimuth from the explosion are shown in Figure 6 and 7. Delay times were determined relative to the center explosion position (Number 2 in Figure 1) and are listed in Table 1. The delay times vary and are less than those for the in-line array.

Since the delay times for this array of stations are less than those for the previously discussed array, a higher band of frequencies 80 to 160 Hz was selected for this profile of stations. This is based on our experience with the previous array where separation was apparent at about 3.5 times the diagnostic frequency (inverse of the input delay times).

The results of the narrow-band filtering are shown in Figures 6 and 7 and are summarized in Table 1. At those stations (2 through 4) where noise was not a problem, the input and observed delay times agree to 1 ms or better.

3.4 DISCUSSION

The significant information derived from this simple experiment are summarized below.

- Accurate relative amplitude and time separation between explosions were achieved at the very close stations and, in particular, at distances less than 1.5 kilometers. Beyond 1.5 kilometers the signal-to-noise ratio is too low in the high frequency band of analysis (required for these separation times) to obtain definitive results.

- Separation between explosions was observed to begin at frequencies 3.5 times the explosion frequency (inverse of the explosion delay times).

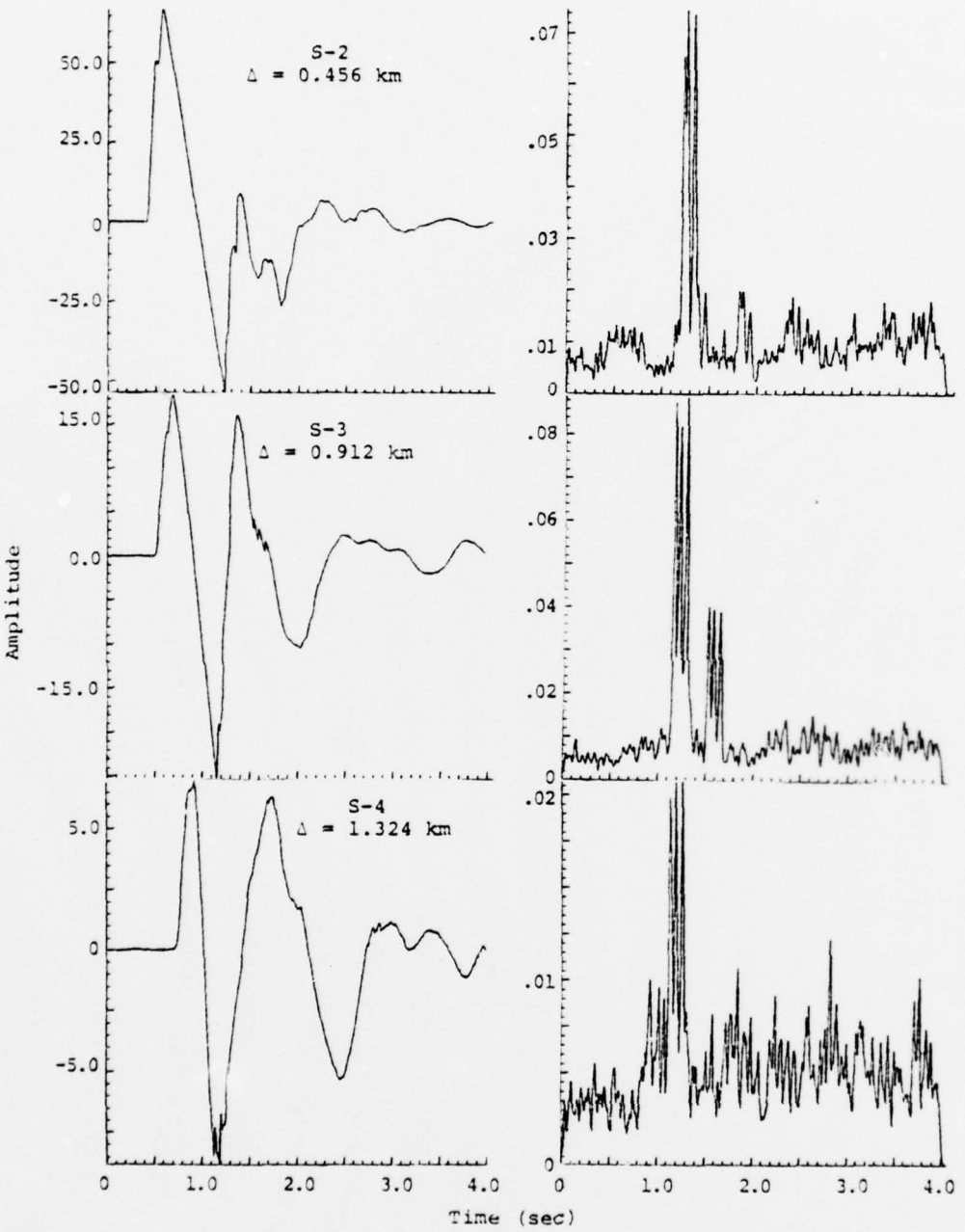

Figure 6. Composite signals and corresponding sum of envelopes for Stations S2, S3 and S4 along the 45° profile shown in Figure 1.

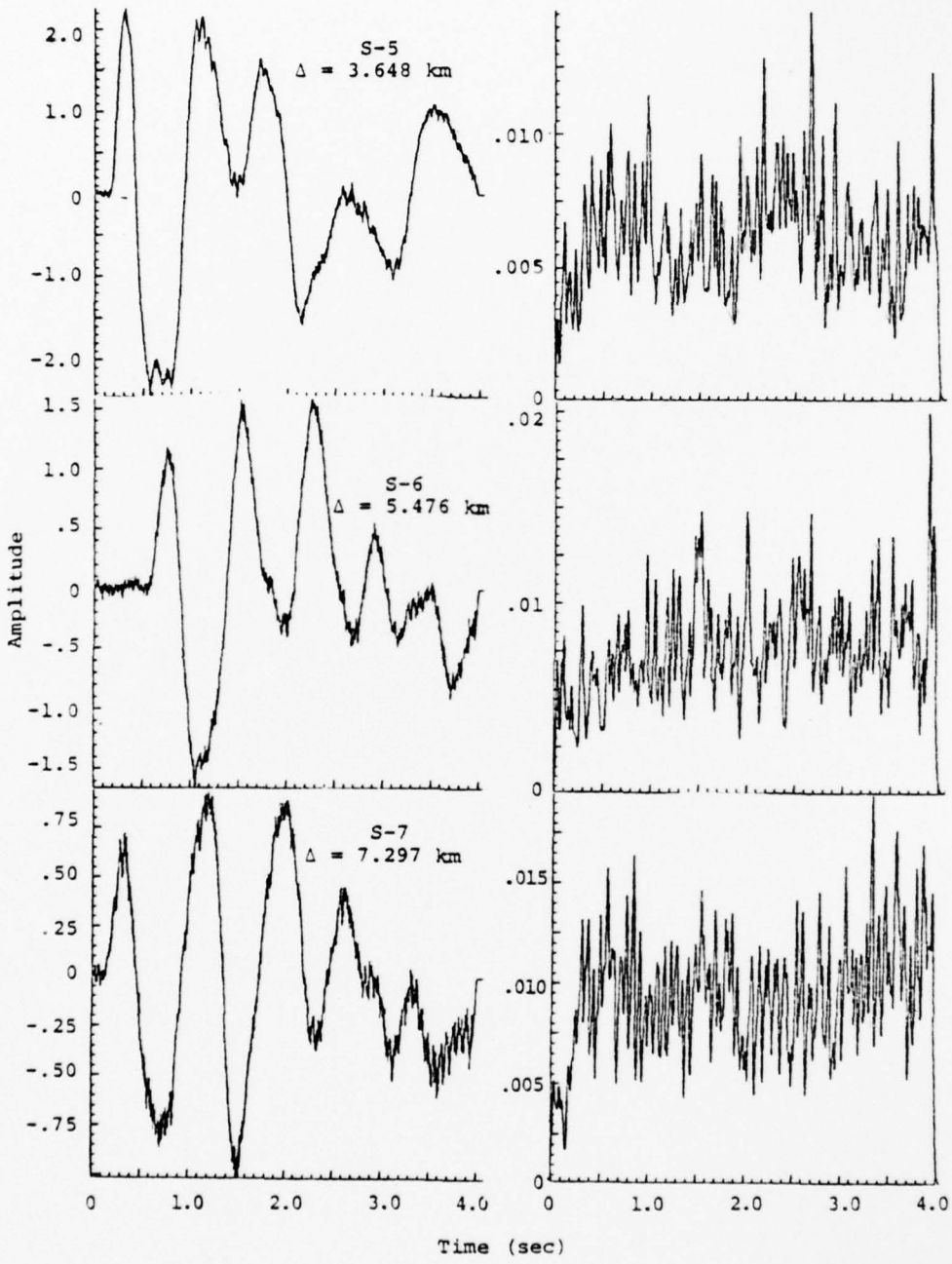

Figure 7. Composite signals and corresponding sum of envelopes for Stations S5, S6 and S7 along the 45° profile shown in Figure 1.

We have described and applied to an example a decomposition method for separating and scaling multiple explosions. However, the example is a simple one and unrealistic in the sense that the propagation path is identical for all events in the series. Further, we have not considered the possibility of one or more of the explosions being time-lagged so that the signal energy arrives at the slapdown time for an earlier event in the sequence. Therefore, even though we were quite successful in detecting and measuring the number and size of the events present for this first example, more realistic simulations are required to confidently judge the usefulness of the technique.

IV. MULTIPLE EXPLOSION SIMULATION - CONSTRUCTION OF COMPOSITE SEISMOGRAMS FROM SEVERAL RECORDINGS OF A SINGLE EVENT

In this section we decompose simulated multiple explosion recordings that are made up from actual recordings of the MAST and COLBY events.

4.1 STATION AND EVENT LOCATIONS

In the previous section we constructed simulated multiple explosion seismograms by delaying and summing individual station records with themselves. By doing so we have assumed that the propagation path effects between individual explosions to one station are negligible. This is probably a good assumption if the explosions are located close together. In this section we use one explosion and a linear array of close-in stations to construct a simulated multiple explosion that includes propagation path effects. To accomplish this we let the explosion position become the point of observation and the station locations become the explosion positions. For example, as in the previous section, we consider a multiple explosion where all of the explosions are detonated simultaneously. In Figure 8a we show part of the actual linear array of close-in stations recording the MAST explosion as well as the travel times (Δt). For the simulation, the station positions become the explosion positions and the MAST explosion location becomes the recording position. A straightforward summation of the station records SZ, S2, S3 and S4 yields a composite signal (Figure 9a) which includes travel path effects between explosions and the observation point. That is, the individual explosions making up the multiple explosion can be considered as being separated by relatively larger distances than those discussed in the

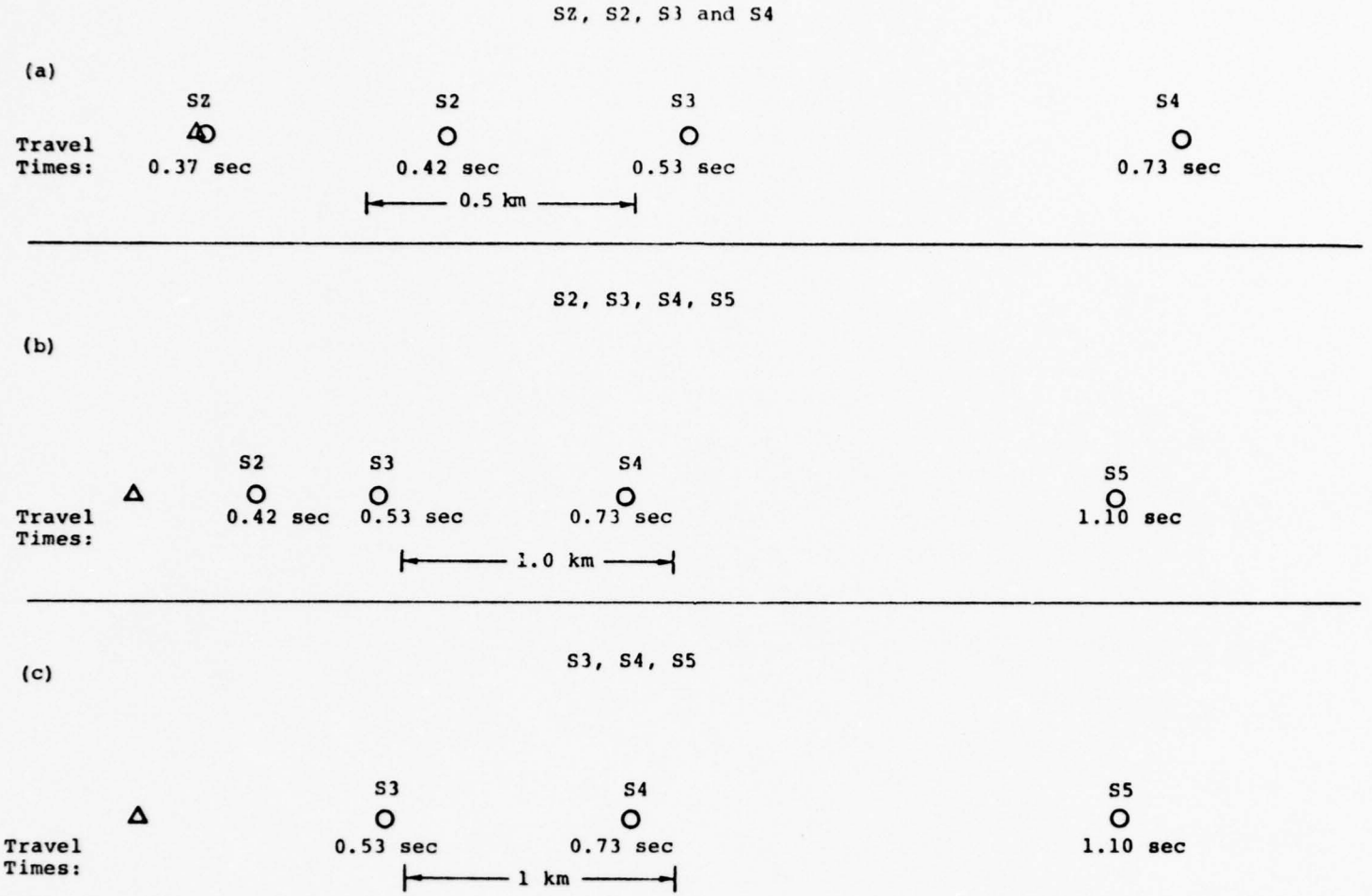

Figure 8. MAST station locations and travel times for Stations SZ, S2, S3, S4 and S5. In a, b and c we show the various combinations of stations used for the construction of three composite signals shown in Figure 9.

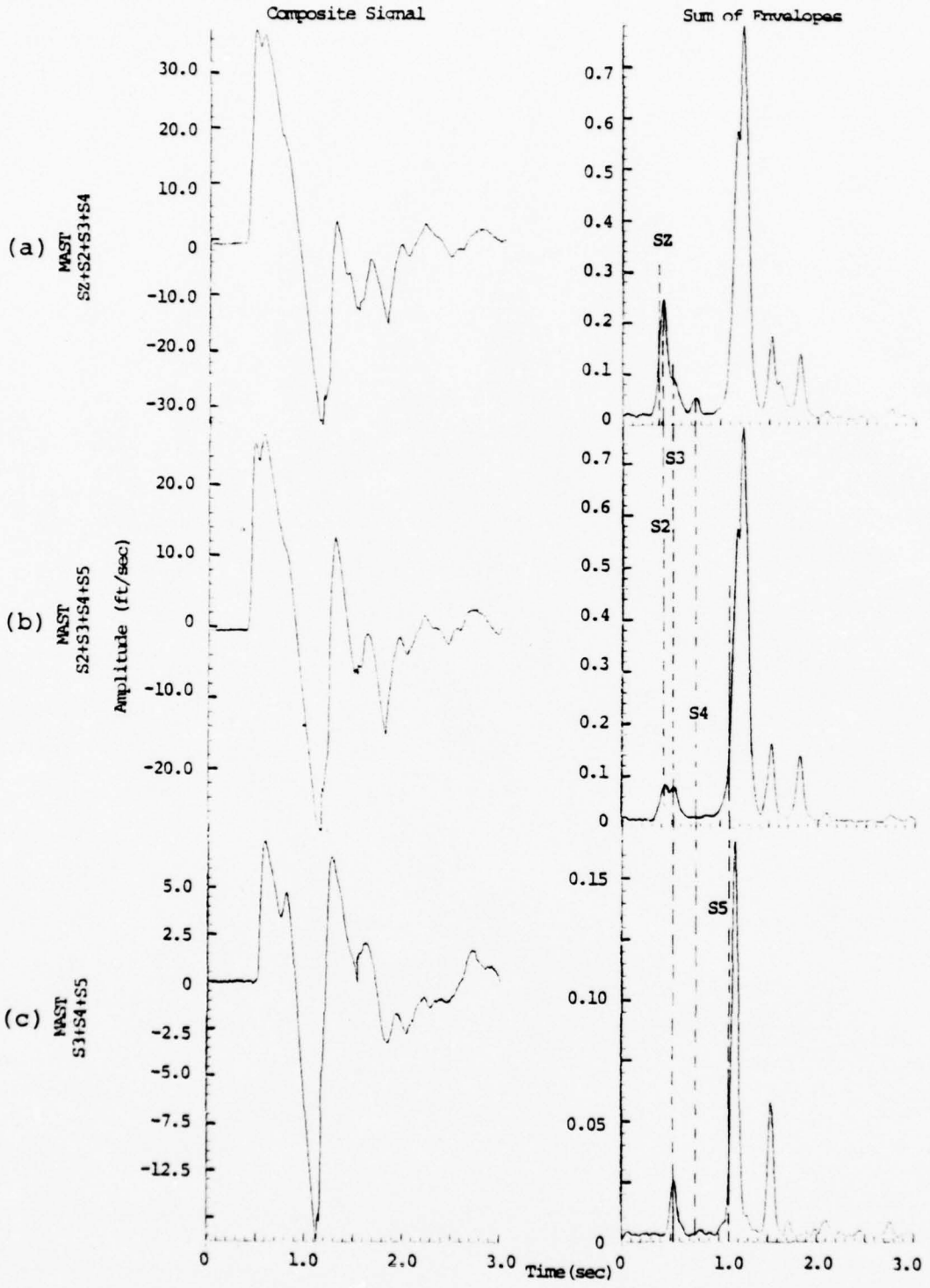

Figure 9. Composite signals and the corresponding sum of the envelopes.

previous section. In the subsections below, we use several different arrays of stations to simulate four multiple explosions. Recordings from MAST and COLBY are used.

Figure 8 shows the explosion and sensor positions as well as the travel times to the explosion for three combinations of seismograms from MAST. The individual records and their horizontal ranges are given in Appendix A. Figure 9 shows the seismograms for the three simulated multiple explosion events shown in Figure 8. All of the multiple event seismograms are significantly different from any of the individual station records used to make them up (Appendix A).

4.2 DECOMPOSITION OF COMPOSITE SIGNALS

Sixteen narrow-band filters with center frequencies ranging from 25 to 100 Hz were applied to the composite signals of Figure 9. The sums of the envelope functions over the specified range of frequencies are shown on the right hand side of Figure 9. We do not see clear separation between individual explosions such as was observed for the previous experiment where we simply delayed and summed the same record to make the composite record. Thus, we are required to carefully examine the individual filter outputs.

Figure 10 is a plot of the envelope amplitude peaks for each narrow-band filter applied to the composite seismogram of Figure 9a. The relative amplitudes are denoted for each filter as indicated in the legend. Useful information is available from only that portion of the signal before the "slapdown" time. The relative complexity of the coda for these composites as compared to those in Section III is mainly due to larger delay times between events. In addition, the energy distribution changes with distance and results in a more complex coda. It is important to note that this is also in contrast to the results in Section III where separation was most clear at the slapdown time.

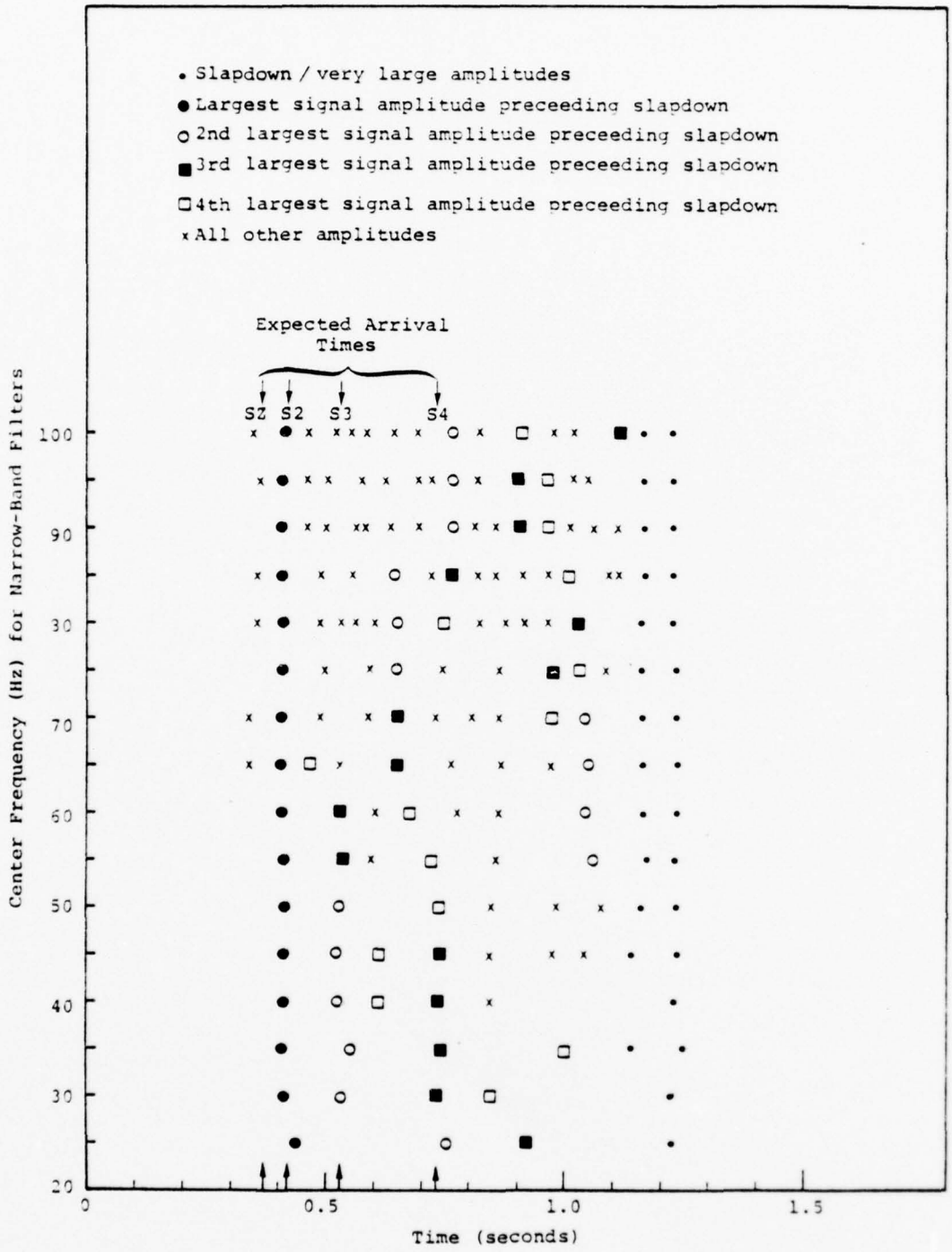

Figure 10. Relative peak filter outputs for the MAST composite seismogram made up from the records SZ, S2, S3 and S4.

Examination of Figure 10 shows three to five possible nondispersed (aligned in time) amplitude peaks. These occur in the frequency range of about 30 to 60 Hz at times of about 0.41, 0.53, 0.73 and, less clearly, at 0.65 and 0.84 seconds. The first three times correspond closely to the expected second, third and fourth (S2, S3, S4) event times for the array and signal of Figures 8a and 9a. The phase at 0.84 seconds consists of small amplitudes but seems to be a bona fide nondispersed phase since it extends to even higher frequencies. The phase at 0.65 seconds also seems real.

From Figure 8a we see that the instrument SZ is located very near (0.015 km) the epicenter. However, the depth of burial is about 0.9 km. The separation or delay time between SZ and S2 is very small, $\approx$ 0.05 seconds. We would expect that these two events should begin to separate at frequencies of about 70 Hz (i.e., 1/0.05 x 3.5 = 70 Hz). A nondispersed small amplitude is visible at a time of about 0.37 seconds between 70 and 100 Hz. This time corresponds closely to the expected arrival time for SZ. However, had we not known to look for an arrival here, we would be unlikely to pick it.

In Table 2 we summarize the data from our analysis of this simulated multiple explosion event. First, we list the pertinent data from the individual records that made up the event. The arrival time is the time from detonation to first motion on the records. The amplitude is the zero-to-peak-amplitude of the first peak. These amplitudes are then normalized to that from S2, the largest amplitude record. For the narrow-band filter output we list the arrival time and relative amplitudes of the arrivals identified as being from separate events. For each arrival the amplitudes were averaged from the N filters from which they were most clearly delineated and this N is listed. The amplitudes were then normalized to that from the arrival at 0.41 seconds.

TABLE 2

SUMMARY OF ANALYSIS OF THE COMPOSITE SIGNAL OF FIGURE 9a (MAST, SZ+S2+S3+S4)

DATA FROM ORIGINAL RECORDS

Station	Arrival Time (sec)	Amplitude (ft/sec)	Normalized Amplitude
SZ	0.37	12.4	0.46
S2	0.42	26.7	1.00
S3	0.53	7.4	0.28
S4	0.73	3.8	0.14

DATA FROM NARROW-BAND FILTER ANALYSIS

Event	Arrival Time (sec)	Normalized Amplitude	N
1*	0.36	0.29	4
2	0.41	1.00	4
3	0.53	0.32	6
4**	0.65	0.19	5
5	0.73	0.24	6
6**	0.84	0.08	8

* Not clearly delineated by the technique.

** Undispersed arrivals that are less prominent than 2, 3 and 5.

There are six arrivals listed in the table of the filter output. Three of these are quite prominent (Figure 10) and in arrival time and relative amplitude correlate with the arrivals represented by S2, S3 and S4. The other event in the composite signal (SZ) is picked from the filter output mainly because we knew when to look for it. Having identified it, the relative amplitude computed agrees fairly well with that of the actual signal. The other two undispersed arrivals tentatively picked by the filters, those at 0.65 and 0.84 seconds, are of smaller amplitude. This casts some suspicion on their validity as evidence of actual events and, together with other information, might be enough to reject them in an actual experiment.

It should also be pointed out that a proper identification of the relative amplitudes of the signals from individual events in a multiple explosion array is the first step in determining the yields, or even the "relative" yields. We must apply some range scaling to remove the path attenuation to determine the actual explosion yields.

In summary the, we have clearly identified the arrival time and relative signal amplitudes from three of the four events making up the multiple explosion. The fourth event is much less clearly identified without some other indication of its presence. Two other possible events are identified by the analytical technique. Here we are using only one piece of information, a single record from a single station, and these two arrivals are only weakly indicated. In an actual experiment additional information (from other stations) would probably be enough to reject these arrivals as evidence of separate explosions.

Using SZ and S2 in the simulated mutliple event, we had arrivals separated in time by only 0.05 seconds. Therefore, we constructed another composite seismogram by leaving out SZ

and adding a more distant station (S5). Figure 8b and 9b show the experimental plan and the composite signal. We see only subtle changes in the composite waveforms between the two simulated events (Figures 9a and 9b).

As before, the sum of envelopes (right hand side of Figure 9b) yields little information for separating events. Thus, it is required that we examine the individual narrow-band filter outputs. Figure 11 shows several possible arrivals. All arrivals appear to be slightly dispersed. The reason for this apparent dispersion is unknown. However, the most prominent arrivals in terms of amplitude appear at 0.42, 0.65, and 1.04 seconds. Less prominent arrivals occur at 0.73 and 0.83 seconds. In Table 3 we summarize the data for this example in the same format as for the previous example (Table 2). However, added weight should be given to the arrivals at 0.42, 0.53, 0.65 and 0.73 seconds, based on the number of frequencies over which each arrival is most clearly delineated. The other two events at 0.83 and 1.04 seconds are not clearly defined over many frequencies.

Summarizing then, we have tentatively identified four events. Three of these event arrival times, 0.42, 0.53 and 0.73 seconds, correspond to three of the four events making up the multiple explosion. The event with the arrival time of 0.65 seconds does not correspond to any known event. Further, we are unable to find a nondispersive peak time of 1.10 seconds which would correlate with the S5 record in the composite signal. This is due to the very small signal from S5 having an arrival time near the slapdown time of S2 and possibly S3.

Dropping the record S2 and summing S3, S4 and S5 we construct another composite record which is simpler than the two discussed above. Figure 8c and 9c show the experimental plan and composite signal. This signal is distinctly different than those shown above (Figures 9a and 9b).

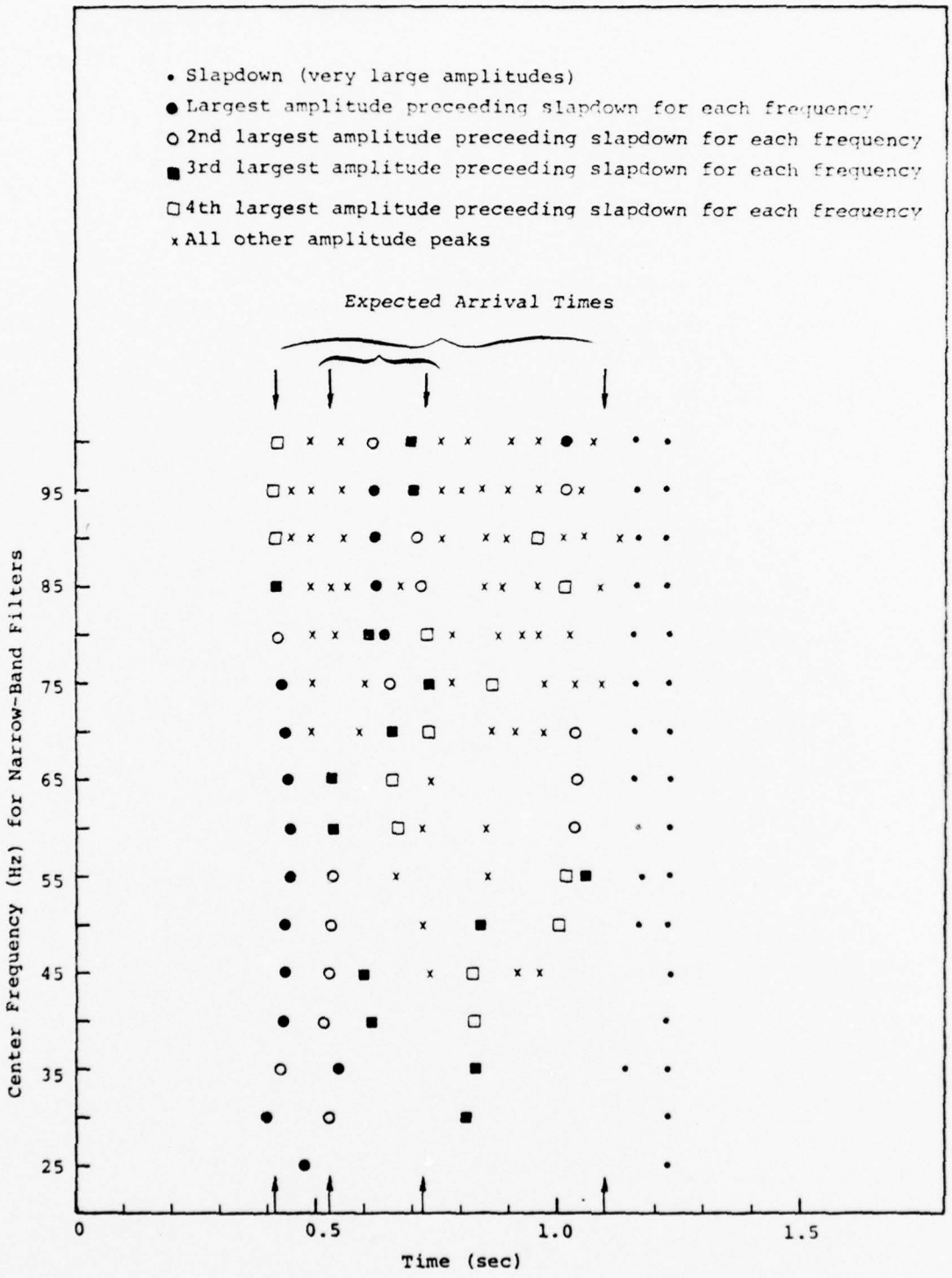

Figure 11. Relative peak filter outputs for the MAST composite made up from Stations S2, S3, S4 and S5.

TABLE 3

SUMMARY OF ANALYSIS OF THE COMPOSITE SIGNAL OF FIGURE 9b (MAST, S2+S3+S4+S5)

DATA FROM ORIGINAL RECORDS

Station	Arrival Time (sec)	Amplitude (ft/sec)	Normalized Amplitude
S2	0.42	26.7	1.00
S3	0.53	7.4	0.278
S4	0.73	3.8	0.141
S5	1.10	1.45	0.085

DATA FROM NARROW-BAND FILTER ANALYSIS

Event	Arrival Time (sec)	Normalized Amplitude	Number of Filters
1	0.43	1.00	7
2	0.53	0.616	7
3	0.65	0.480	5
4	0.73	0.156	7
5	0.83*	0.190	6
6	1.04*	0.660	4

* Undispersed arrivals less prominent than 1, 2, 3 and 4.

Examination of the individual narrow-band filter output (Figure 12) shows several possible nondispersed waveforms. The most clear arrivals are at 0.53 and 0.73 seconds. Less prominent arrivals occur at 0.60, 0.80, 0.90 and 1.04 seconds. The latter four are not clearly defined as being nondispersed while the former two are clearly arriving at the same time over many frequencies.

Table 4 summarizes the data for this example in the same format as for the previous two examples (Tables 2 and 3). There are six arrivals listed in Table 4, two of which are prominent (Figure 12) and in arrival time and relative amplitude correlate with the arrivals represented by S3 and S4. Again we are unable to detect the small event S5 that should arrive at 1.10 seconds. The S5 event has an arrival time corresponding closely to the slapdown phase of S3. This amplitude dominates the record at this time and masks the small S5 event.

4.3 DISCUSSION

We have identified various prominent and less prominent arrivals from the decomposition of three simulated explosion arrays. Correlation of these results (Tables 2, 3 and 4) show prominent arrivals that correlate in time and amplitude with the events S2, S3 and S4. However, there are situations in which we are unable to separate all events. In the simulation in which it is included, SZ is separated by only 0.05 seconds from S2 and cannot be identified. In another simulation the small event S5 occurs during the slapdown phase for an earlier event.

In Figure 9, we showed and have discussed the individual composite signals. On the right hand side of the figure we show for the corresponding composites the sum of 16 envelope functions for the frequency range of 25 to 100 Hz. In such an alignment of envelope sums, common explosion peaks become

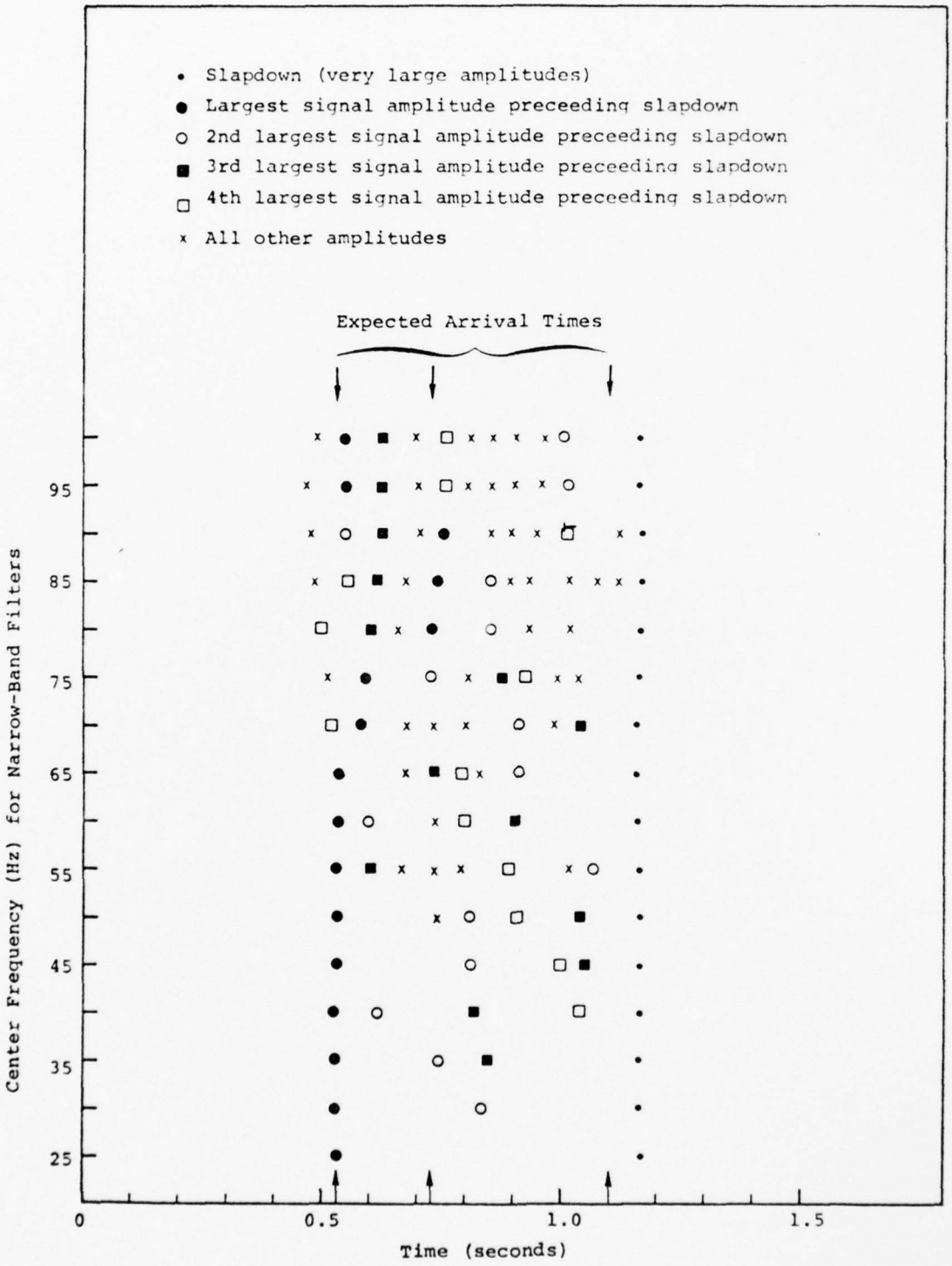

Figure 12. Relative peak filter outputs for the MAST composite made up from Stations S3, S4 and S5.

TABLE 4

SUMMARY OF ANALYSIS OF THE COMPOSITE SIGNAL OF FIGURE 9c (MAST, S3+S4+S5)

DATA FROM ORIGINAL RECORDS

Station	Arrival Time (sec)	Amplitude (ft/sec)	Normalized Amplitude
S3	0.53	7.4	1.00
S4	0.73	3.8	0.514
S5	1.10	1.45	0.196

DATA FROM NARROW-BAND FILTER ANALYSIS

Event	Arrival Time (sec)	Normalized Amplitude	Number of Filters
1	0.53	1.00	6
2*	0.60	0.270	3
3	0.73	0.412	6
4*	0.80	0.191	6
5*	0.90	0.243	4
6*	1.04	0.282	4

* Undispersed arrivals that are less prominent than 1 and 3.

simpler to correlate as we can see from Figure 9 where most of the events are in common. Correlation over a network of stations would improve our capability for detecting and scaling individual events in a multiple explosion.

4.4 RESULTS OF THE COLBY ANALYSIS

In the second of the three experiments discussed in the previous subsection, MAST Stations S2, S3, S4 and S5 were used to construct the multiple explosion record. We were unable to identify the most remote "event", S5. To further pursue the questions this raises, a similar composite signal was constructed using station records S3, S4, S5 and S6 from COLBY (Appendix A). COLBY is considerably larger in yield than MAST and the signal-to-noise ratios at the more distant stations should be relatively greater.

Figure 13 shows the alignment of stations and appropriate travel times. Figure 14 presents the simulated multiple explosion and the sum of the envelopes from 16 narrow-band filters. The sum of the envelopes yields little information for the separation of individual events. Therefore, we need to examine the individual narrow-band filter outputs. In Figure 15 we have plotted the envelope amplitude peaks for each narrow-band filter applied to the composite seismogram. Three prominent peak amplitudes are apparent corresponding closely in time to the expected times. Further, and perhaps more importantly, a peak begins to separate out from the slap-down phase for most distant (5.182 km) event (S6).

Table 5 presents a summary of the analysis of the COLBY composite signal. The computed relative amplitudes vary from the actual values by factors of 2.4, 2.9 and 19.4. The last ratio (19.4) is associated with the S6 event. This large amplitude is most likely due to constructive interference from the explosion slapdown phase.

	S3	S4	S5	S6
Travel Times:	0.47	0.64	0.89	1.35

○ EXPLOSIONS (i.e., actual station records for S3, S4, S5 and S6 become explosion positions).

△ SENSOR LOCATION (i.e., actual explosion position becomes the sensor position).

Figure 13. COLBY station locations and travel times for Stations: S3, S4, S5 and S6.

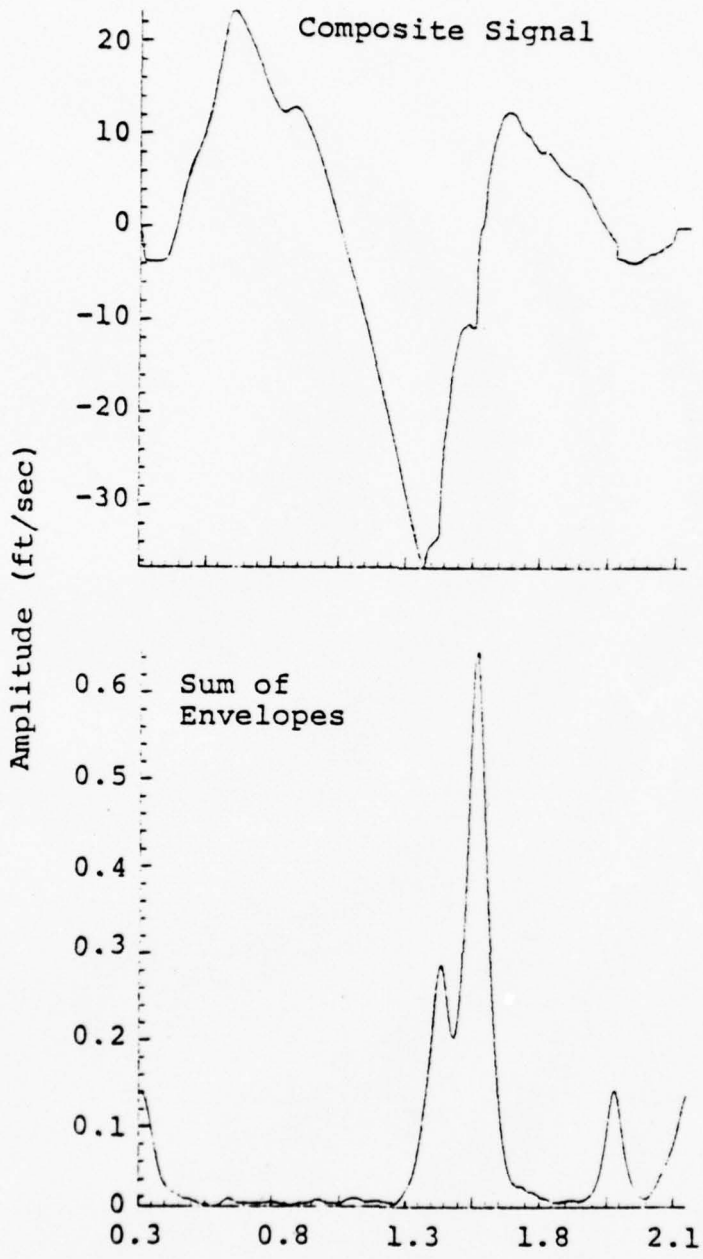

Figure 14. Composite signal for COLBY and the corresponding sum of the envelopes.

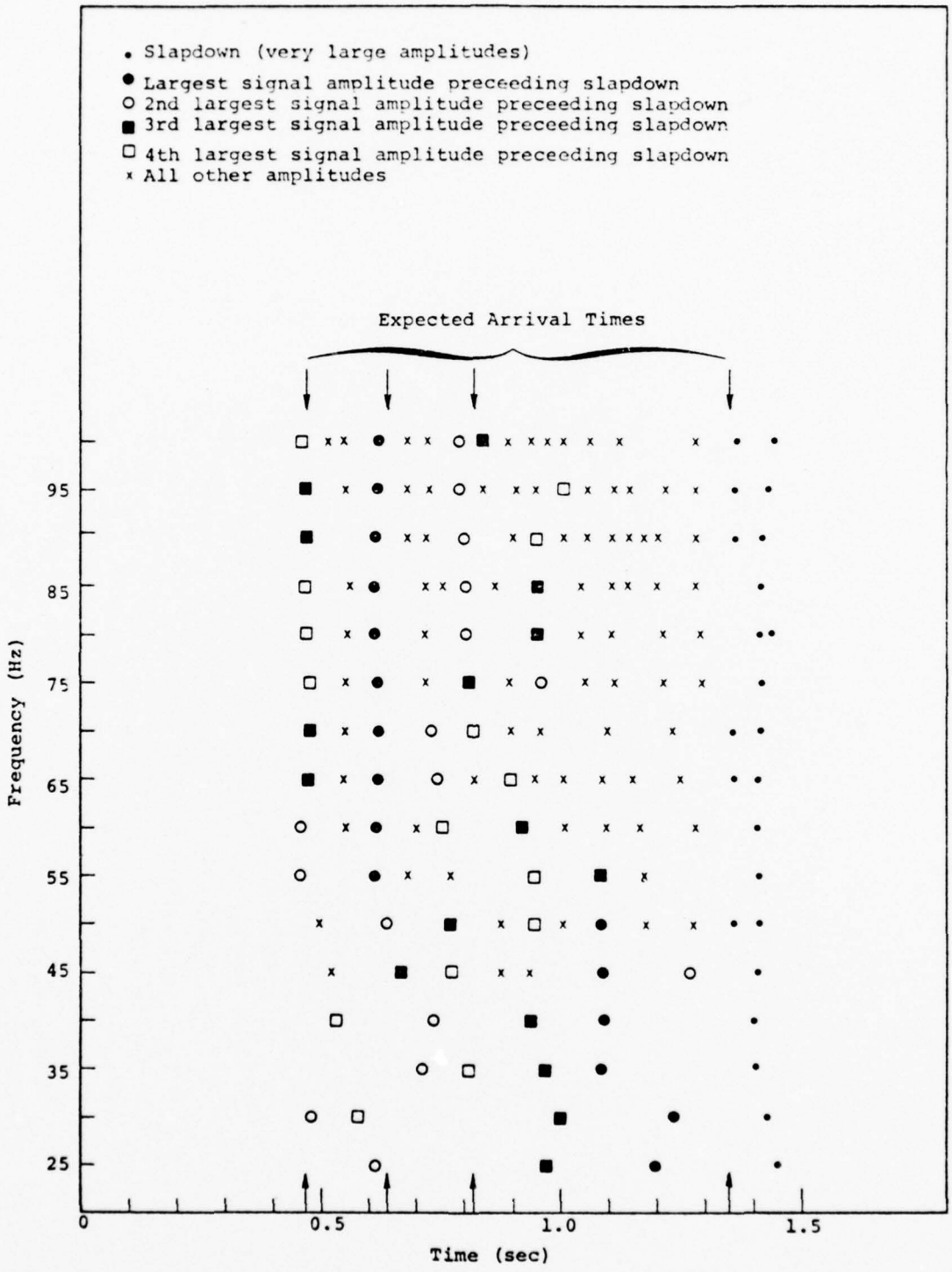

Figure 15. Relative peak filter outputs for the COLBY composite made up from Stations S3, S4, S5 and S6.

TABLE 5

SUMMARY OF ANALYSIS OF THE COMPOSITE SIGNAL OF COLBY

(S3+S4+S5+S6)

DATA FROM ORIGINAL RECORDS

Station	Arrival Time (sec)	Amplitude (ft/sec)	Normalized Amplitude
S3	0.47	15.3	1.00
S4	0.64	13.4	0.786
S5	0.82	5.4	0.353
S6	1.35	2.3	0.150

DATA FROM NARROW-BAND FILTER ANALYSIS

Event	Arrival Time (sec)	Normalized Amplitude	Number of Filters
1	0.47	1.00	9
2	0.62	1.873	9
3	0.80	1.01	8
4	1.36	2.91	6

The analytical results are no better than those for the comparable MAST example, in fact, the amplitude relationships are not as good.

4.5 SUMMARY

Utilizing a linear array of close-in station records for MAST and COLBY, we simulated multiple explosions which include propagation path effects. This is accomplished by assuming all explosions (station recordings) occurred simultaneously and summing the station records. Thus, the real explosion point now becomes the observation point and the station positions become the explosion positions.

The important results obtained from this study are as follows:

- The complexities of the later portions of the composite seismograms (i.e., slapdown times and later) increased when compared to the previous simpler experiment (Section III). This prevented using the later portion of the record for analysis.

- When an event first arrival occurs during the slapdown phase from the earlier event, we are unable to detect or identify that event.

- When the separation between event arrivals is quite small, less than 0.1 seconds, it is difficult to unambiguously identify the event.

- We are able to separate and identify the signals from the largest (or closest) of the events in the multiple explosion array. The arrival times are correctly picked within 0.02 seconds and the computed relative amplitudes are well within a factor of two of the actual values.

- A number of additional arrivals are tentatively picked by the narrow-band filter technique. Some of these correspond to actual arrivals from smaller or more remote events while some do not correspond to individual events. Other information must be used to tell which of these is evidence of an actual explosion.

- Records from other near-field stations should considerably increase the resolution. An array of stations is needed to confidently detect and scale the individual events making up the multiple explosion.

V. MULTIPLE EXPLOSION SIMULATION - CONSTRUCTION OF A COMPOSITE SEISMOGRAM FROM VARIOUS EVENT SEISMOGRAMS

The use of close-in seismograms for several explosions allows the construction of more complex simulated multiple explosion seismograms than those of Sections III and IV. In particular, the propagation path is more different for the different events.

5.1 STATION AND EVENT LOCATIONS

In Figure 16 we show a linear array of stations made up of COLBY, POOL and MAST records. These records include stations S2 and S4 for COLBY, S9 for POOL and S3 for MAST. However, the propagation path for MAST (S3) is entirely different from the others. Thus, the MAST event, realistically, should be considered to lie outside the linear array and could be located at any azimuth about the hypothetical receiver position. On the other hand, since the POOL (S9) station and COLBY (S2, S4) stations actually lie in a straight line between the two events (COLBY and POOL), some similarities in the overall propagation path are probable. Thus, a realistic positioning of POOL (S9) can be either as shown in Figure 16 or rotated 180° from where shown. Based on the results from Section IV, explosions (station records) were chosen such that first arrival times occur before the slapdown time for the closest event. We again assume that all explosions occur simultaneously and sum the indicated station records.

5.2 DECOMPOSITION

Sixteen narrow-band filters in the frequency range of 25 to 100 Hz were applied to the composite signal shown in

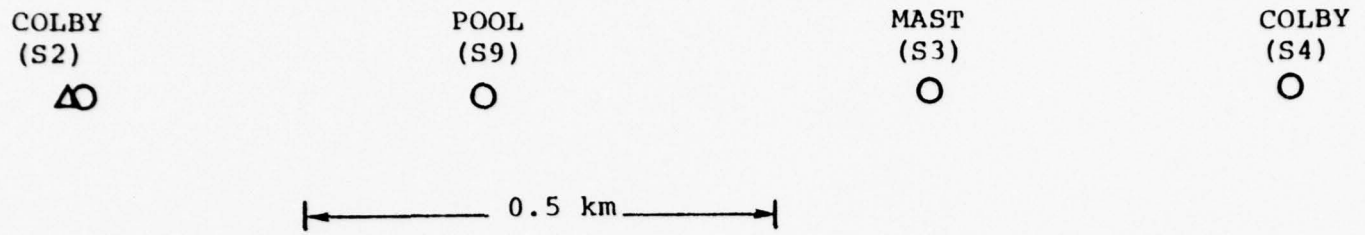

Travel Times:	0.29	0.42	0.53	0.64

O Explosions (all explosions occur at the same time).

Δ Sensor location

Figure 16. COLBY (S2) + POOL (S9) + MAST (S3) + COLBY (S4). Station locations and travel times.

Figure 17. The sum of the envelope functions over the specific range of frequencies is shown on the right hand side of this figure.

In general, we observe that the composite signal is distinctly different from any single station seismogram (Appendix A). The envelope sums do show peaks at the expected times. However, separation and scaling must be attempted with care. This is particularly true since the complexity of the coda increases. Thus, as in the MAST and COLBY experiments, described in Section IV, only the nondispersed filter peaks near the beginning of the signal are evidence of separate events. In Figure 18 we show the envelope peaks for each filter. It is clear that the four peaks that correspond to those in the sum of envelopes (Figure 17) are prominent non-dispersed waves. Less prominent nondispersed waves may be present and would require additional information to identify them.

5.3 RESULTS AND DISCUSSION

In Table 6 we summarize for comparison the measured travel times and amplitudes. Travel times compare with 0.02 seconds and relative amplitudes within a factor of two with the exception of MAST (S3). The calculated amplitude is 3.3 times greater than the expected one for this event. At this point we are uncertain as to the cause or causes for this large difference. These differences could be due to such things as:

- Amplitude enhancement due to constructive interference with some phase from an earlier event.

- Higher dominant signal frequency content for MAST due to differing geophysical source or path characteristics from those of COLBY and POOL.

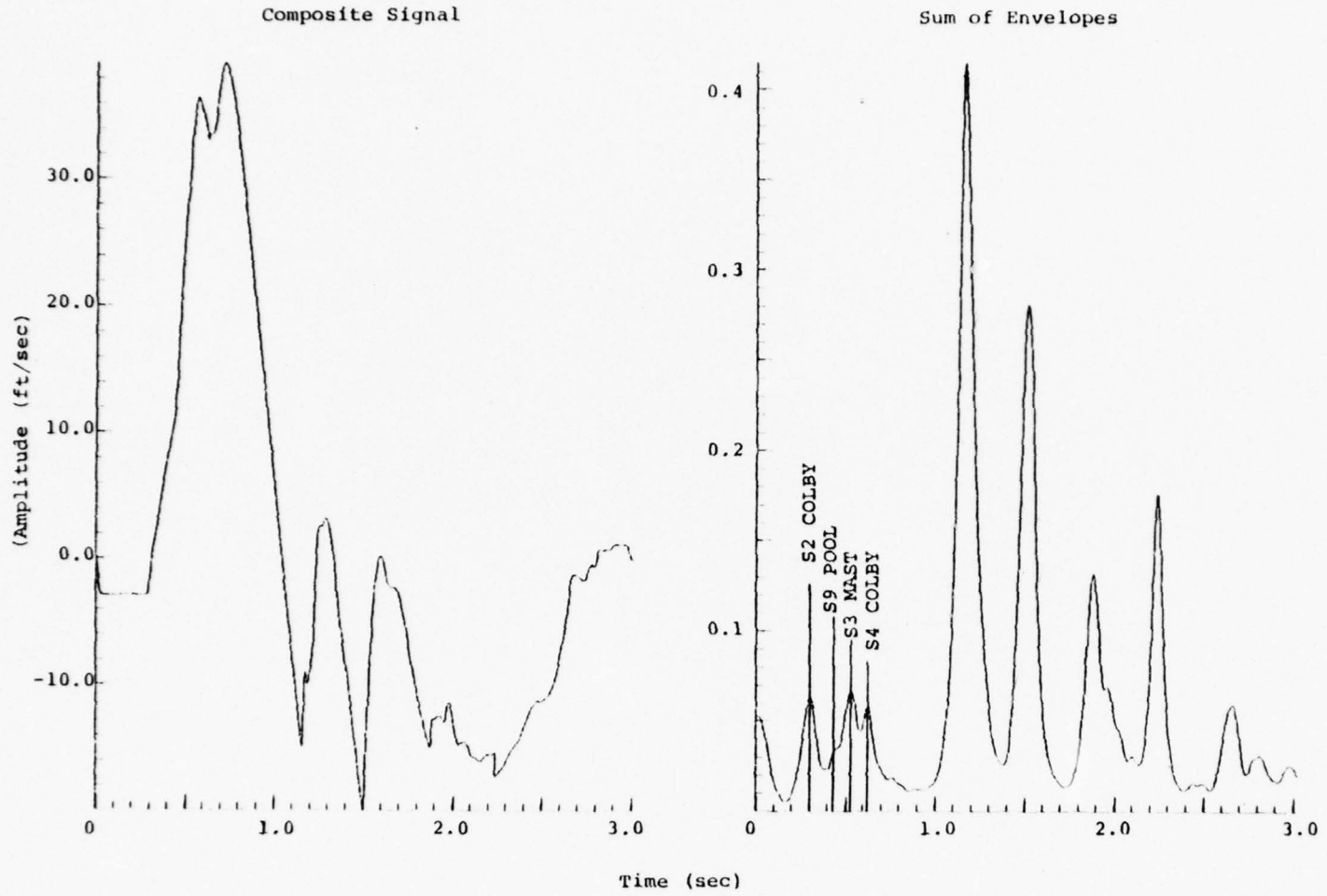

Figure 17. Composite record and corresponding sum of envelopes for COLBY (S2) + POOL (S9) + MAST (S3) + COLBY (S4).

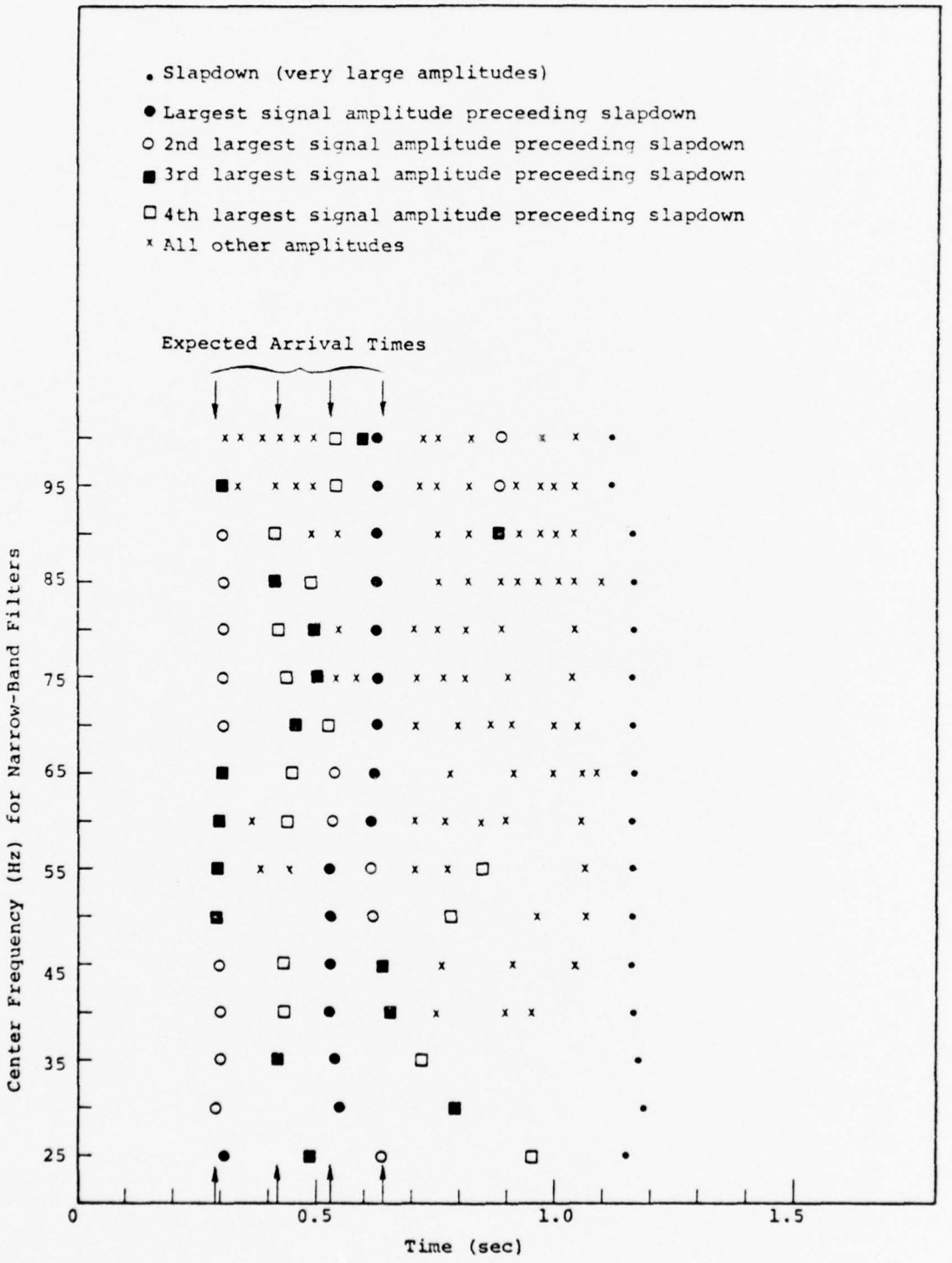

Figure 18. Relative peak filter outputs for the composite made up from Stations S2 and S4 (COLBY), S9 (POOL) and S3 (MAST).

TABLE 6

SUMMARY OF ANALYSIS OF THE COMPOSITE SIGNAL OF

COLBY (S2) + POOL (S9) + MAST (S3) + COLBY (S4)

DATA FROM ORIGINAL RECORDS

Station	Event	Arrival Time (sec)	Amplitude (ft/sec)	Normalized Amplitude
S2	COLBY	0.29	20.0	1.000
S9	POOL	0.42	12.7	0.635
S3	MAST	0.53	7.4	0.370
S4	COLBY	0.63	12.3	0.615

DATA FROM NARROW-BAND FILTER ANALYSIS

Event	Arrival Time (sec)	Normalized Amplitude	Number of Filters
1	0.301	1.00	10
2	0.432	0.516	10
3	0.534	1.230	10
4	0.628	1.130	10

Whatever the cause, these uncertainties in amplitude estimations must be known to determine the degree of confidence that can be placed on the relative amplitude estimates and, ultimately, yield estimation.

5.4 SUMMARY

Using close-in station records from several events (COLBY, POOL and MAST), we have simulated a multiple explosion event consisting of three events in a linear array and one outside this array. This simulation includes real propagation path differences. Based on the results obtained in the previous section (V), we required all explosions to have first arrival times earlier than the slapdown time for the closest event for the purpose of detecting the events.

The important results are as follows:

- Filter or envelope peaks do occur at the expected times and are within 0.02 seconds of these expected times.

- Comparison of relative amplitudes are within a factor of two except for the event outside the array. Here the amplitude is 3.3 times greater than the expected one.

- We do not know the reason for this factor of 3.3. However, if it were possible to simulate an array of stations for this example, then perhaps a more accurate determination of the relative amplitude could be made.

VI. MULTIPLE EXPLOSION SIMULATION - CONSTRUCTION OF COMPOSITE SEISMOGRAMS FROM A TELESEISMIC RECORDING

In all of the previous work we have dealt with close-in seismic recordings which retain considerable high frequency signal energy (i.e., energy in the range of 25 to 100 Hz). In this section we are concerned with the problem of decomposing teleseismic signals with the use of narrow-band filters. Teleseismic signal recordings will contain little high frequency signal energy relative to the close-in recordings. We will show the usable frequency range for teleseismic signals to be about 0.3 to 3.5 Hz.

6.1 CONSTRUCTION OF COMPOSITE SEISMOGRAMS

From the previous work (Section III) we found that separation of events was possible with filter frequencies of about 3.5 times the explosion frequency (i.e., inverse of the time differences between explosions) and became increasingly clear with increasing frequencies. It turns out that the minimum time delay that we can expect to resolve using teleseismic data is greater than about 1.0 second. That is, the signal energy is low at frequencies greater than 3.5 Hz and we would not expect to be successful in separating events having delay times less than 1.0 second.

The simulation of composite signals is the same as for those described in Section III. That is, we use one seismogram delayed in time and summed with itself. For this purpose, a teleseismic recording of MAST at station E was selected. Three composite seismograms, each consisting of three events, are formed. The left hand side of Figure 19 shows the original MAST seismogram (top left) and the three

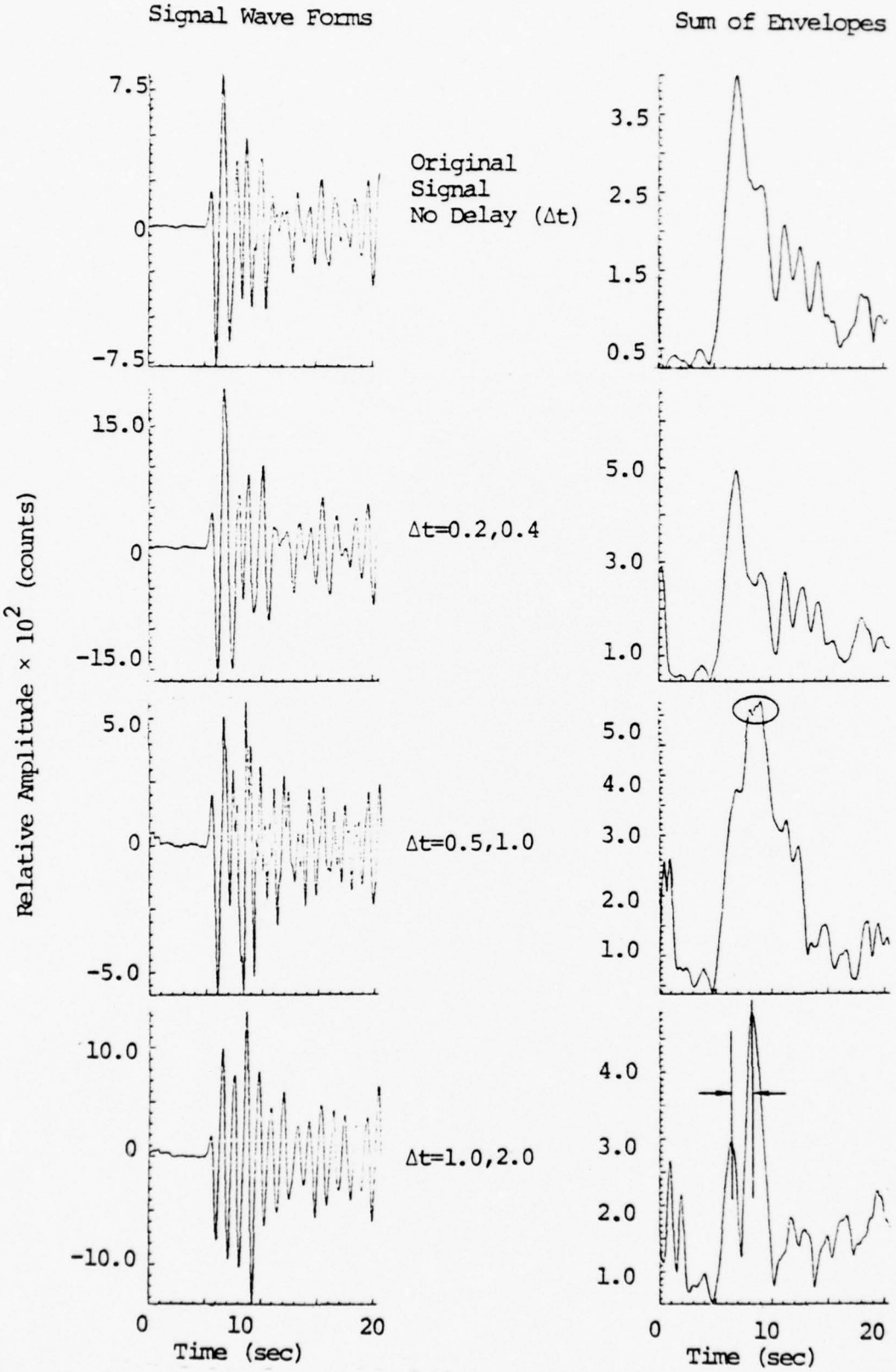

Figure 19. Original and composite signal wave forms and the sum of envelopes for a MAST teleseismic record.

composites aligned below with corresponding delay times (Δt) indicated to the right of each composite waveform. Delay times between 0.4 and 2.0 seconds were chosen to test the criteria discussed above.

6.2 DECOMPOSITION OF MAST TELESEISMIC COMPOSITE SIGNALS

Fifteen narrow-band filters for frequencies from 3 to 10 Hz were applied to the original and composite signals of Figure 19. For signals dominated by frequencies of 1 Hz, the lowest filter frequency that would seem useful is about 3 Hz. The highest frequency (10 Hz) represents the Nyquist frequency. The sums of the envelope functions over the specified range of frequencies are shown on the right hand side of Figure 19. Both the signal waveform and the sum of the envelopes of the original signal show the complexity of the signal coda. The sum of envelopes shows various peaks in the coda which may be attributed to other unidentified body wave arrivals.

The first composite signal has delay times of 0.2 and 0.4 seconds. As we expected, for these small delays we do not find separation of the three events.

The second composite signal has delay times of 0.5 and 1.0 second. Again, we did not expect to find any definitive separation. However, the composite wave form shows distinct high frequency interference. The peak of the envelope sums shows the suggestion of three small peaks separated in time by 0.5 seconds (see circled portion of envelope maximum). However, from careful inspection of the individual filter outputs as a function of frequency we cannot state with confidence that these three peaks are nondispersed body phases.

The third composite signal has delay times of 1.0 and 2.0 seconds. The sum of envelopes shows two peaks separated in time by two seconds. These peaks correspond in time to

the amplitude peaks of the first and third event in the composite. Examination of the individual filter outputs shows that there are two large peaks separated in time by two seconds for only the lowest filter frequency (3.0 Hz). There is no evidence of corresponding peaks at higher frequencies nor is there evidence of peaks corresponding to the expected time for the event lagged 1.0 seconds. The filter output and envelope sum thus indicate rather clearly that there are two events. Scaling of these two events by the relative peak amplitudes will be obscured by interference from the one second lagged event.

6.3 DISCUSSION

On the basis of these results for teleseismic data it seems clear that narrow-band filtering cannot identify with confidence nondispersed body waves separated in time by much less than 2.0 seconds. In the example with two second separation, only one filter (3.0 Hz) out of the 15 in the frequency range of 3.0 to 10 Hz provided the required information for separation. The explanation for these results becomes obvious when viewing the amplitude spectra of the original MAST signal (Figure 20). At 3.0 Hz the amplitude of the signal is two orders of magnitude below the peak and at 4.5 Hz the amplitude is down by three orders of magnitude from the peak. Thus, for this example little usable signal information is present at frequencies greater than 3.0 Hz.

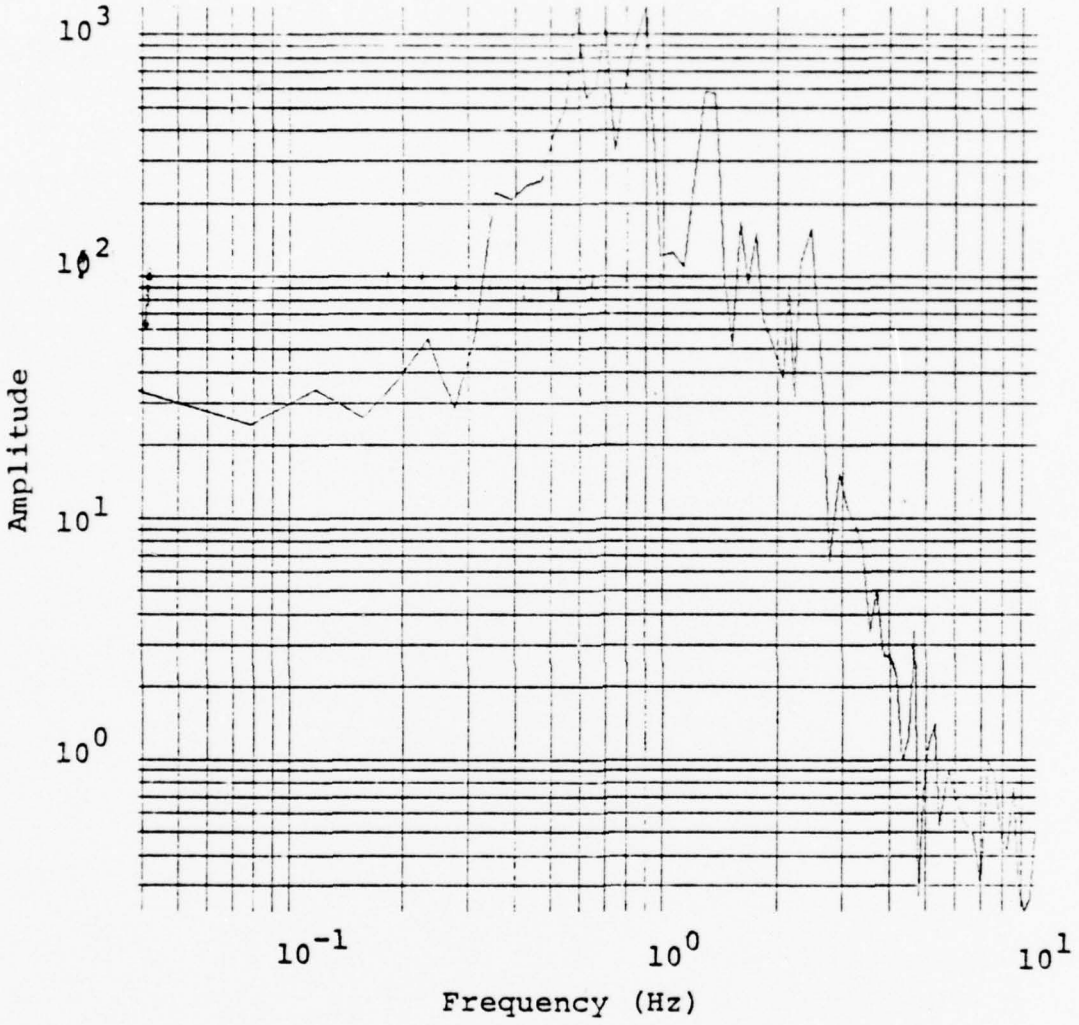

Figure 20. Amplitude spectra for MAST Station E.

VII. SUMMARY AND DISCUSSION

Our objective in this study has been to develop analytical procedures for using seismic measurements to determine the number and size of individual explosions making up multiple explosion events. Further, we want to test the capability to detect explosions detonated concurrently with a multiple explosion event but located outside the explosion array.

7.1 ANALYTICAL PROCEDURES

The analytical procedures used to decompose (separate and scale) multiple explosions observed at close-in distances make use of a series of narrow-band filters (Appendix B). These filters separate the time series into a set of quasi-harmonic modulated "signals." The use of these narrow-band filters is predicated on the fact that there is high frequency energy present in the close-in seismograms. The frequency range required lies somewhere above the explosion frequency. The explosion frequency is defined as T^{-1}, where T is the delay time between primary arrivals from the individual explosions comprising a multiple event.

Our results show that using narrow-band filters, the separation of the individual events of a multiple explosion begins at about 3.5 times the explosion frequency and becomes more clear with increasing frequency until the signal-to-noise ratio approaches unity. Thus, the placement of appropriate detectors for monitoring multiple explosions must be made with consideration of the above criteria. Very simply, this means that the detectors located nearest the multiple event provide the best chance for the successful separation and scaling of the individual explosions comprising a multiple event.

7.2 ANALYTICAL RESULTS

Basically, we have investigated three kinds of simulated multiple explosions. The first kind can be considered to be comprised of an array of three closely-spaced, equal-sized explosions observed along two close-in station arrays (Section III). For these composites we summed the individual station seismograms with themselves. Thus, we did not account for any path differences between the individual explosions and the receiver. In Section VI we investigate similar multiple explosions recorded at teleseismic distances.

The second kind of multiple event can be thought of as an array of four widely-spaced, equal-sized explosions observed at one close-in station. For this experiment the actual explosion location becomes the observation point and the recording station array represents the explosion array (Section IV). Use of these seismograms as explosions incorporates the propagation path differences between the various sources. It is important to note that the signals at individual stations along the array from MAST and COLBY do change significantly with distance (Appendix A).

The third multiple event configuration is similar to the second one discussed above in that we exchange the explosion positions with actual station seismograms. However, we input different explosion records and hence change the propagation path effects and explosion yields (Section V). This third multiple event configuration can be envisioned in two ways. The first is that of a widely spaced three explosion array and an explosion located outside this array. It can also be considered as one explosion located at some point away from a linear array of three explosions and the observation point located in line with the linear explosion array. (See Figure 16 and attendent explanation in Section 5.1.)

Application of the narrow-band filtering techniques to these simulated multiple explosions yielded the following results:

- For the closely spaced explosion array, accurate separation and relative scaling of events is achieved at stations close to the multiple event. However, at more distant stations, the signal-to-noise ratio is too low in the frequency band of analysis to achieve definitive results.

- For the closely spaced explosion array recorded at teleseismic distances, separation of events with less than 2.0 second delays was not achieved. Basically, the technique is constrained by the lack of the required high frequency signal energy at teleseismic distances.

- For the widely spaced explosion arrays, the complexities of the later portions of the composite seismograms (i.e., slapdown times and later) increased as compared to the closely spaced explosion composite. Further, when one event first arrival occurred during the slapdown phase from an earlier event, we were not able to detect or identify that first arrival.

- For the widely spaced explosion arrays, separation of events is achieved by analyzing the first portion of the composite signal. Accurate separation of events is obtained for those detected. Scaling of the detected events gives relative amplitudes varying by about a factor of two from the expected values for most events. Occasionally, larger deviations may occur and these are probably due to interference

from other signal phases. This amplitude error would be much less if we had several stations recording the event.

- For the third multiple event configuration we obtain similar results to that described for the second configuration (widely spaced explosion arrays). However, the relative scaling of the event outside the three explosion array is too large by a factor of 3.3. This is most likely due to constructive interference. However, an array of stations is needed to resolve this question.

7.3 DISCUSSION

Several limitations are imposed in attempting to simulate multiple explosions from seismograms from a single explosion. These are as follows:

- For widely spaced explosions we are unable to realistically simulate a multiple explosion at more than one station. Thus, it is not possible to evaluate with confidence the degree with which an array of stations will aid in the scaling problem. However, an array of stations can be of great aid in identifying individual events by correlating times from one record to another.

- Forming a realistic reverse profile is also not possible due to the fact that we cannot account for propagation path effects. However, in one sense we do this in the experiment where we use several different explosions (Section V).

- Summation of individual seismograms increases the high frequency energy content. The presence of additive high frequency noise most likely makes it more difficult to separate the desired events.

Despite these difficulties it seems clear that closely spaced explosions (in time) can be identified and scaled. Further, an array of stations would probably greatly improve the capability to identify the individual explosions making up a multiple explosion.

The design of this station array should be based upon the expected spatial and temporal configuration of the planned multiple explosion. Station positions should be determined such as to maximize the expected time differences between individual explosions. Also, stations should be located as close as is practical to the multiple explosion location for recording high frequency signal energy. The presence of high frequency signal energy is fundamental to the success of the analytical technique.

VIII. REFERENCES

Lambert, D. G., C. F. Peterson and J. M. Savino, [1976] "Explosion Yield Verification, Multiple Explosion Scenarios and Three-Dimensional Seismic Modeling Research," Systems, Science and Software Quarterly Technical Report, AFTAC/VSC, SSS-R-76-2993, August 1976.

Savino, J. M., T. C. Bache, T. G. Barker, J. T. Cherry, D. G. Lambert, J. F. Masso, N. Rimer and W. O. Wray, [1976], "Improved Yield Determination and Event Identification Research," Systems, Science and Software Final Report, AFTAC/VSC, SSS-R-77-3038, October 1976.

Bache, T. C., J. T. Cherry, K. G. Hamilton, J. F. Masso and J. M. Savino, [1975], "Application of Advanced Methods for Identification and Detection of Nuclear Explosions From the Asian Continent," Systems, Science and Software Semi-Annual Report, SSS-R-75-2646.

Savino, J. M., T. C. Bache, J. T. Cherry, K. G. Hamilton, D. G. Lambert and J. F. Masso, [1975], "Application of Advanced Methods for Identification and Detection of Nuclear Explosions From the Asian Continent," Systems, Science and Software Semi-Annual Technical Report SSS-R-76-2792.

APPENDIX A

VELOCITY SEISMOGRAMS FROM THE EVENTS MAST, COLBY, AND POOL

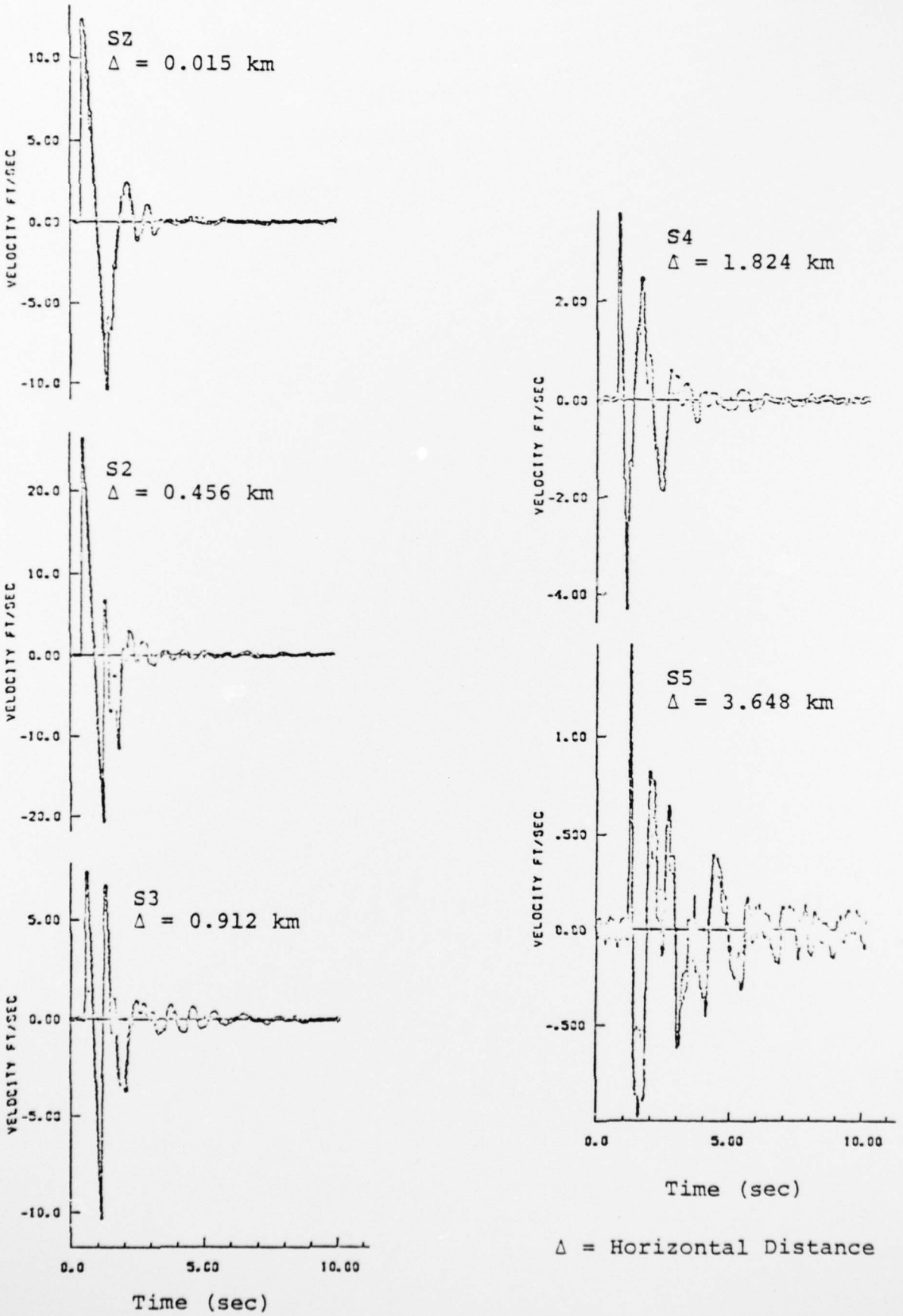

Δ = Horizontal Distance

MAST SEISMOGRAMS

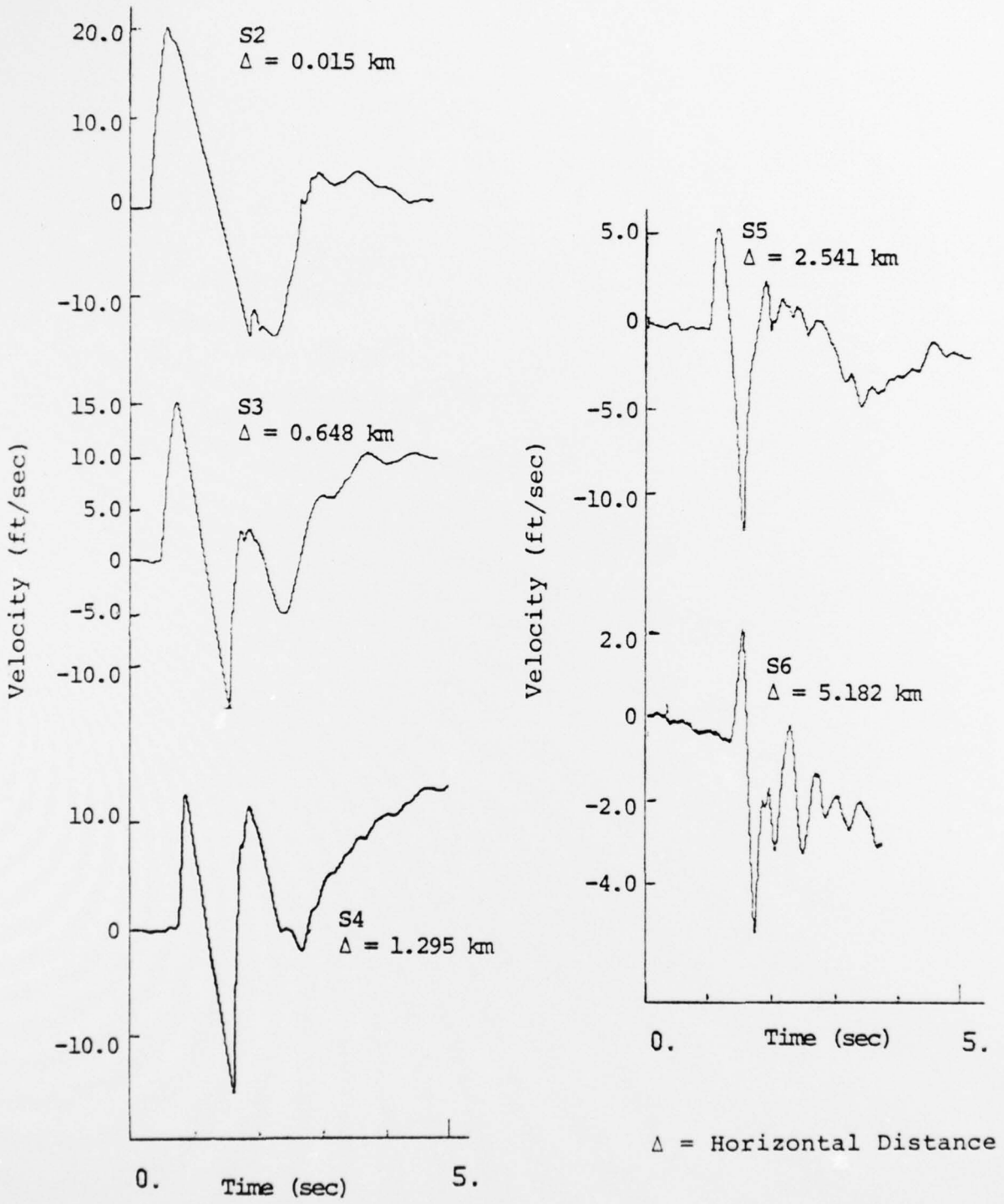

COLBY SEISMOGRAMS

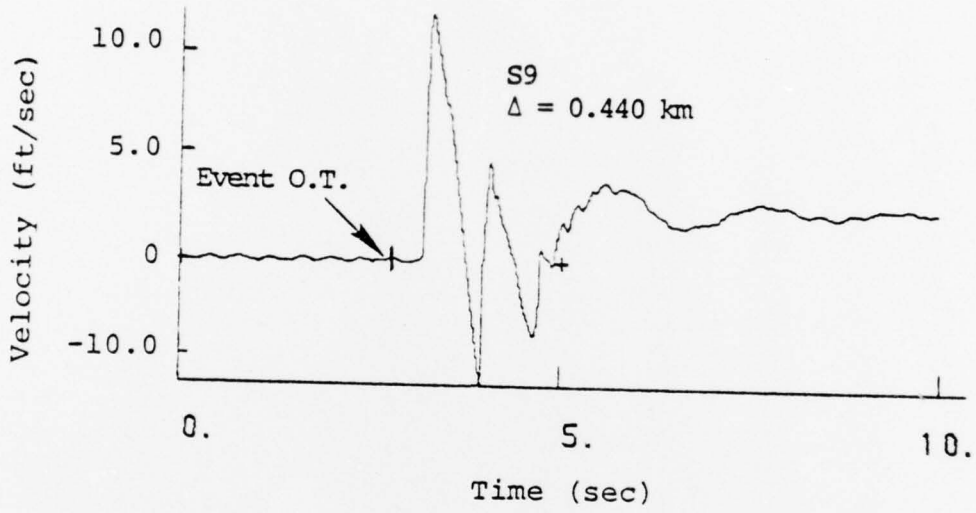

O.T. = Origin time
Δ = Horizontal distance

POOL SEISMOGRAM

APPENDIX B

SIGNAL ANALYSIS PROCEDURE

Decomposition of a complex time series can be accomplished with the use of a series of narrow-band filters. These filters separate the time series into a set of quasi-harmonic modulated "signals." This procedure was adopted in the MARS signal analysis program employed for this experiment and can be used to separate and scale multipe explosion scenarios as long as there is sufficient energy (good signal-to-noise ratio) at frequencies greater than T^{-1} Hz. Here, T is the delay time between primary arrivals recorded at a particular sensor from individual explosions comprising a multiple event.

Figures A.1 and A.2 are two different versions of the flow of operations in the MARS signal analysis program. Figure A.1 gives a verbal outline while Figure A.2 summarizes the key mathematical operations performed in this program. More detailed descriptions of the theory and operation were presented in Bache, et al., [1975] and Savino, et al., [1975].

Seismic data are read into MARS in the form of a time series generally of about 500 to 2000 points in length. The data are then optionally detrended, mean removed and tapered at the tail end by a cosine bell. The program then selects the smallest power of two which is greater than the number of points input and performs a discrete Fourier transform using the algorithm of Cooley and Tukey [1965]. Both the original time series and the spectrum are plotted for examination.

Referring to Figures A.1 and A.2, the signal is next filtered in the frequency domain by multiplication with a narrow-band cusp-shaped filter of the form:

$$F(f) = \begin{cases} 1 - \cos \frac{\pi}{3} \left[\frac{f - \left(f_c - \frac{3}{2} \Delta f \right)}{\Delta f} \right], & f_c - \frac{3}{2} \Delta f \leq f \leq f_c \\ 1 - \cos \frac{\pi}{3} \left[\frac{\left(f_c + \frac{3}{2} \Delta f \right) - f}{\Delta f} \right], & f_c \leq f \leq f_c + \frac{3}{2} \Delta f \\ 0, \text{ otherwise} . \end{cases}$$

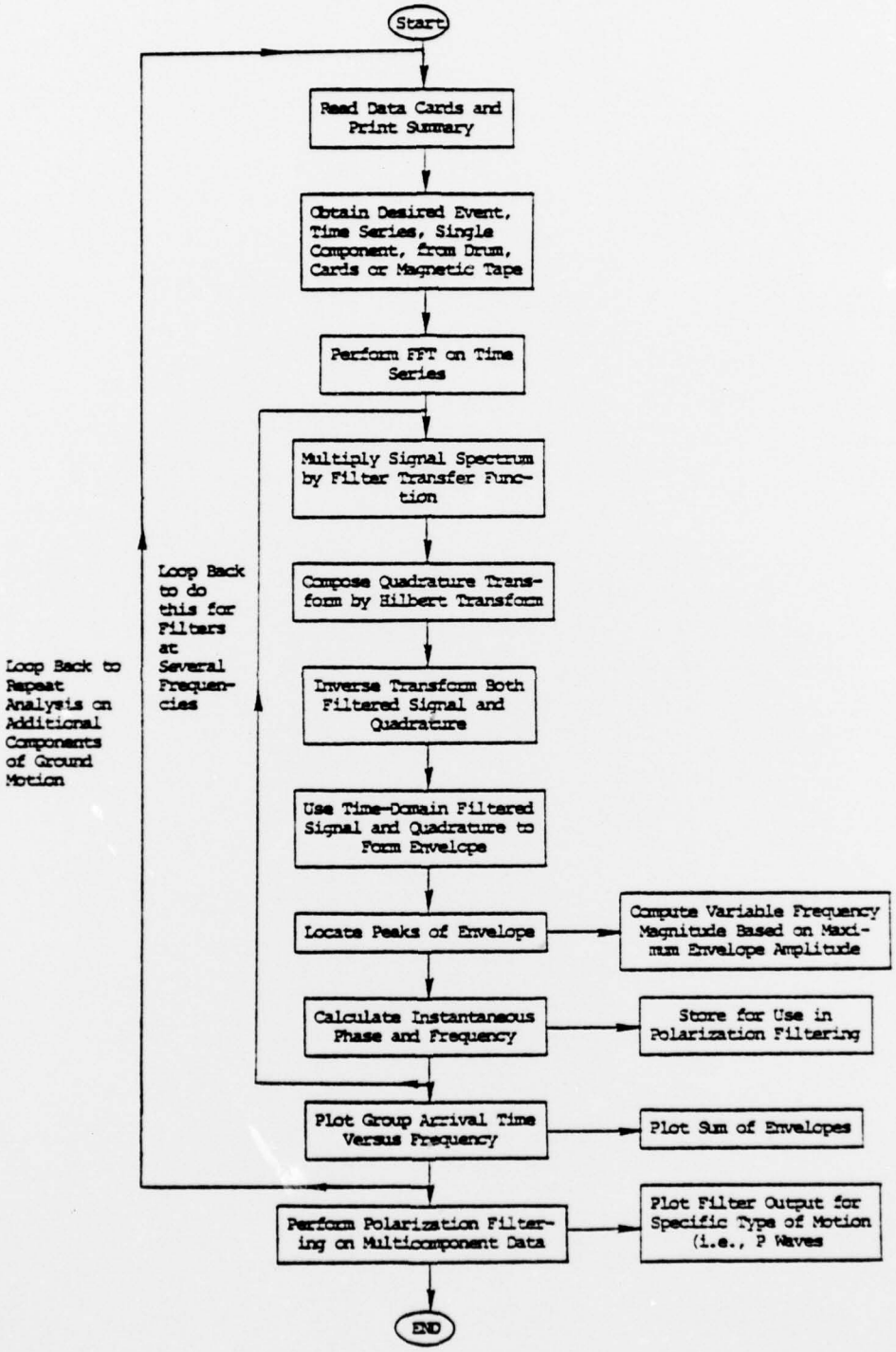

Figure A1. MARS flowchart.

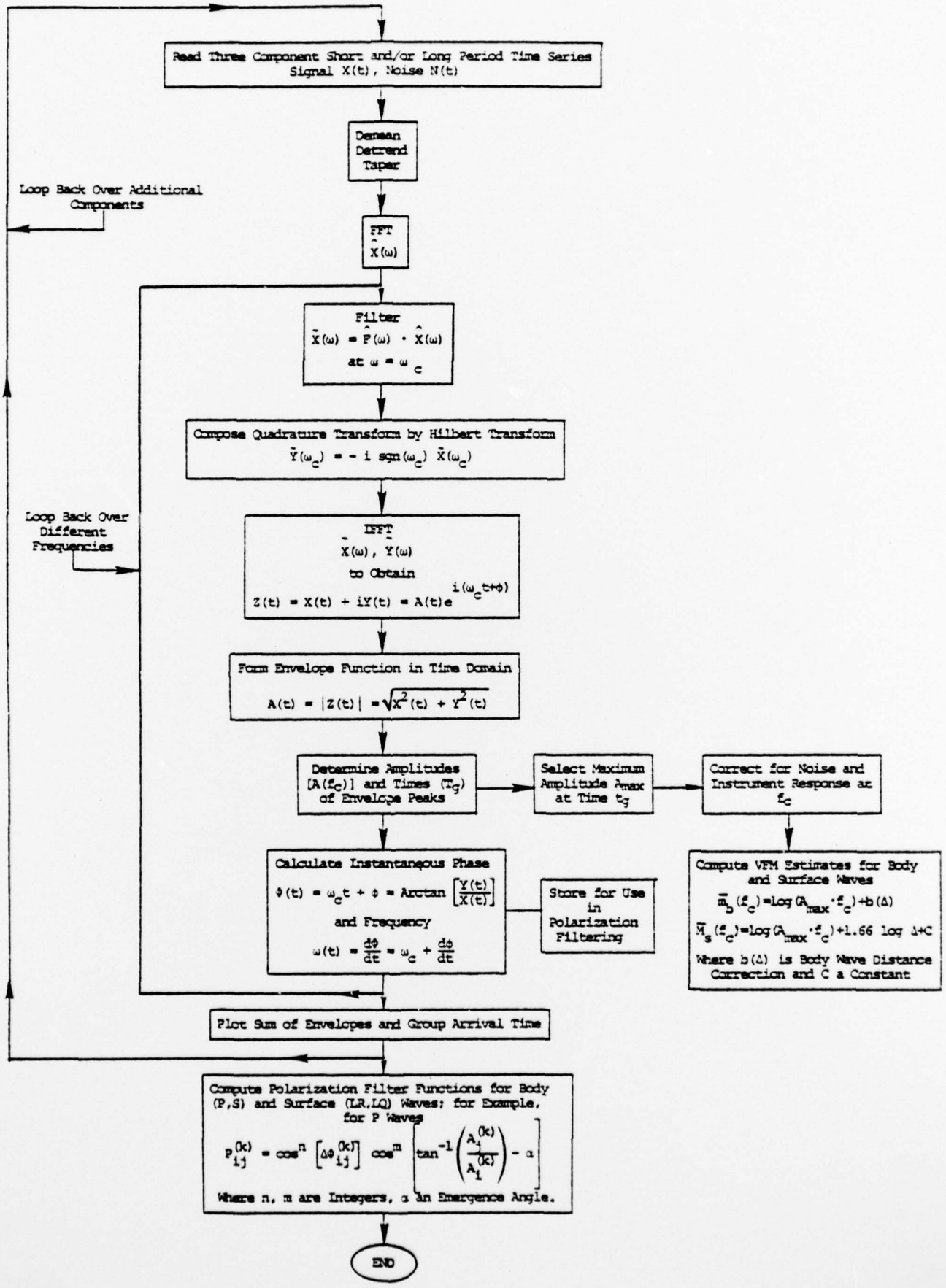

Figure A2. Flowchart indicating principal mathematical operations embodied in the MARS program.

This particular filter form, shown in Figure A.3, was selected to satisfy two goals: (1) minimum width in the frequency domain, and (2) maximum ripple suppression in the time domain. A well-known consequence of the Uncertainty Principle (Sampling Theorem to electrical engineers) is that one cannot simultaneously satisfy these two goals to arbitrary precision. The filter employed was selected for its optimal time and frequency domain characteristics within the limits of the Uncertainty Principle.

Once the signal has been narrow-band filtered, it is corrected for the appropriate instrument response; the filtered signal transform is divided by the instrument transfer function. The resulting complex spectrum is then inverse Fourier transformed into the time domain, to produce what will hereafter be referred to as the filtered signal.

The narrow-band filtered signal will appear as a quasi-sinusoidal carrier wave contained within a smooth envelope. The next step in the program (Figures A.1 and A.2) is to construct the envelope function by means of the Hilbert transform. This method is followed in MARS: the transform of the filtered signal is multiplied by $-i\ \mathrm{sgn}(\omega)$ and then brought to the time domain by an inverse transformation. The maximum of the envelope function is utilized for $m_b(f)$ estimates while the instantaneous frequency and phase are stored for subsequent use in polarization filtering with additional components of ground motion.

The narrow-band filtering procedure can be performed on a particular component seismogram (time series) at a number of different frequencies within some band of interest. Correlation of the resulting envelope functions indicates the arrival times of the various frequency components. Examples of the separation of different phase arrivals that can be achieved by the narrow-band filtering procedure in MARS are described in the results of multiple explosion experiments.

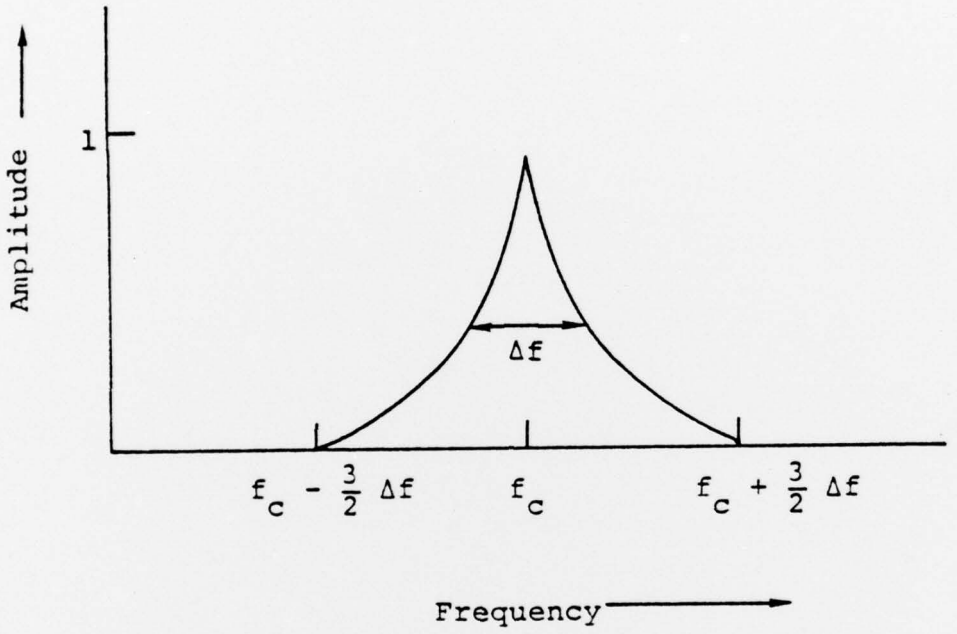

Figure A3. Narrow-band filter used in MARS. The width at one-half maximum amplitude is designated Δf and for this experiment is set equal to 0.2.